

**The effect of *Vesicular stomatitis virus* and *Herpes simplex virus* infection on  
the expression patterns of p63 and Bax in epithelial cell lines**

László Orosz M.D.

Ph. D. Thesis

2010.

**The effect of *Vesicular stomatitis virus* and *Herpes simplex virus* infection on the expression patterns of p63 and Bax in different epithelial cell lines**

László Orosz M.D.

Ph.D. thesis

Department of Medical Microbiology and Immunobiology,  
University of Szeged, Faculty of Medicine

2010.

**LIST OF PUBLICATIONS*****Full papers cited in the thesis***

- I. Megyeri, K., Orosz, L., Kemény, L. (2007). Vesicular stomatitis virus infection triggers apoptosis associated with decreased  $\Delta Np63\alpha$  and increased Bax levels in the immortalized HaCaT keratinocyte cell line. *Biomed. Pharmacother.* **61**, 254-260. IF: 1.526
- II. Megyeri, K., Orosz, L., Kormos, B., Pásztor, K., Seprényi, G., Mándi, Y., Bata-Csörgő, Z., Kemény, L. (2009). The Herpes simplex virus-induced demise of keratinocytes is associated with a dysregulated pattern of p63 expression. *Microb. Infect.* **11**, 785-794. IF: 2.51
- III. **Orosz, L.**, Gallyas, É., Kemény, L., Mándi, Y., Facskó, A., Megyeri, K. (2010). Involvement of p63 in the *Herpes simplex virus-1*-induced demise of corneal cells. *J. Biomed. Sci.* **17**:47.

**ABBREVIATIONS**

ABTS	2,2'-azino-bis(3-ethylbenzthiazoline-6-sulphonic acid)
ATM	ataxia teleangiectasia mutated pathway
ATR	ataxia teleangiectasia mutated- and rad3-related pathway
Bax	Bcl-2-associated X protein
Bcl-2	B-cell lymphoma 2
BH	Bcl-2 homology
BSA	bovine serum albumin
DBD	DNA-binding domain
DDR	DNA damage response
DNA	deoxyribonucleic acid
EDTA	ethylenediaminetetraacetic acid
EF	enrichment factor
ELISA	enzyme-linked immunosorbent assay
FACS	fluorescence-activated cell sorter
FITC	fluorescein isothiocyanate
gD	glycoprotein D
hpi	hour(s) postinfection
HSV	<i>Herpes simplex virus</i>
IFN	interferon
kDa	kiloDalton
LAT	latency-associated transcript

M	matrix protein
MAb	monoclonal antibody
MOI	multiplicity of infection
MTT	3-(4,5-dimethylthiazol-2-yl)2,5-diphenyltetrazolium bromide
N	nucleocapsid
Oct	octamer binding protein
OD	oligomerization domain
p53 <sup>mt</sup>	mutated p53
p53 <sup>wt</sup>	wild-type p53
PAGE	polyacrylamide gel electrophoresis
PBS	phosphate-buffered saline
PFU	plaque forming unit
PI	propidium iodide
PIKK	phosphatidylinositol 3-kinase-like kinase
PKR	double-stranded RNA-dependent protein kinase
RNA	ribonucleic acid
SAM	sterile alpha motif
SD	standard deviation
SDS	sodium dodecyl sulfate
SIRC	Staatens Seruminstiute Rabbit Cornea cell line
SiRNA	short interfering RNA or silencing RNA
TA	transactivation
TID	transactivation inhibitory domain
$\alpha$ -TIF	$\alpha$ -trans-inducing factor

UV	ultraviolet radiation
vhs	virion-associated host shutoff protein
VSV	<i>Vesicular stomatitis virus</i>

## INTRODUCTION

During the course of their replication, viruses perturb many strictly monitored cellular processes, and the profound structural and functional damage eventually kills the infected cells [1-5]. The demise of virus-infected cells may play a pivotal role in the pathogenesis of diseases by destroying the structural and functional integrity of human tissues. Moreover, the cytopathogenicity of viruses defined as viral oncolytic therapy agents can be exploited in the treatment of malignant tumors [6-9]. The tissue damage triggered by viruses involves various forms of cell death, including necrosis, apoptosis, anoikis, pyroptosis, necroptosis and autophagy [1, 2, 10-18].

Necrotic cell death is characterized by cytoplasmic and organelle swelling, followed by the loss of cell membrane integrity and release of the cellular contents into the surrounding extracellular space. The activation of necrosis is important for virus-induced inflammation and innate immune control of viral infections [19].

Apoptosis is a form of cell death characterized by cell shrinkage, chromatin condensation, chromosomal DNA fragmentation, plasma membrane blebbing and formation of apoptotic bodies. These morphological changes are consequences of the activation of specific enzymes, called caspases, which mediate the execution phase of apoptosis [19]. Apoptosis of host cells during viral infection functions as a defense mechanism by destroying the site of pathogen replication [19, 20]. Nevertheless, apoptosis is subverted by many viruses to ensure their replication [19-21].

Anoikis is programmed cell death induced by a loss of cell adhesion [19, 22]. Extracellular matrix receptors of the integrin family play an important role in anoikis suppression [22]. The cells respond to detachment from the extracellular matrix by disruption of the actin skeleton, leading to cell rounding and the triggering of anoikis via activation of pro-apoptotic Bcl-2 family proteins and the mitochondria-mediated apoptotic pathway [19, 22]. This kind of apoptosis following the loss of cell anchorage is important for development, tissue homeostasis and several diseases, such as cancer [19, 22].

Pyroptosis is a more recently recognized form of regulated cell death, with morphological and biochemical properties distinct from necrosis and apoptosis [19, 23]. Active caspase-1, the central executor of pyroptotic cell death, acts mainly by inducing the formation of discretely sized ion-permeable pores in the plasma membrane. The resulting osmotic pressure leads to water influx, cell swelling and ultimately cell lysis. Furthermore, caspase-1 activation initiates an inflammatory response by cleavage of the proinflammatory cytokines pro-interleukin-1 $\beta$  and pro-interleukin-18, which are released by the cell upon their

activation [19]. Pyroptosis plays an important role in cell death during the course of infectious diseases [23].

Necroptosis is a process of regulated cell death displaying necrotic morphology, which can be induced by death domain receptors through receptor-interacting protein-1 kinase activity [19, 24]. Although necroptosis is activated by the same stimuli as those that initiate apoptosis, the morphological features of this kind of cell death (organelle swelling, rapid mitochondrial dysfunction, plasma membrane permeabilization and a lack of nuclear fragmentation) are characteristic of pathological necrosis, which is presumed to be unregulated death caused by overwhelming stress [19, 24].

Autophagy is an evolutionarily conserved catabolic pathway that allows eukaryotes to degrade and recycle cellular components [19]. Proteins and organelles are sequestered in specialized double-membrane vesicles, designated autophagosomes [19]. Many viruses have been shown to evade, subvert or exploit autophagy, seemingly to ensure their own replication or survival advantage [25]. Autophagy in virus-infected cells may be accompanied by other modes of cell death, or it may be involved in the sensitization of infected cells to apoptosis or exert an inhibitory effect on apoptotic cell death evoked by viral infection [19].

## **I. Herpes simplex viruses**

The Herpes simplex viruses (HSV-1 and HSV-2), which belong in the *Herpesviridae* family, are 120-200 nm in size. The virions are composed of a double-stranded DNA genome of about 150 kbp, a capsid shell with 162 capsomers, a protein layer termed the tegument on the outside of the capsid, and an outer envelope composed of viral membrane proteins and glycoproteins embedded in a lipid bilayer [1]. The genome contains two covalently linked components, one long and one short, with unique sequences such as unique long and unique short, flanked by large inverted repeats. These viruses encode at least 84 different polypeptides, which serve several hundred functions [1, 2, 26].

To initiate infection, virions attach to different classes of cell surface molecules, including heparan sulfate chains on proteoglycans, a member of the tumor necrosis factor receptor family (herpesvirus entry mediator) and two members of the immunoglobulin superfamily (nectin-1 and nectin-2) [27]. Thereafter, the virions fuse their envelope with the plasma membrane. Once inside the cell, HSVs appear to use the intracellular transport machinery to accomplish targeting to the nucleus. After the nucleocapsid reaches the nuclear pores, the viral DNA translocates into the nucleoplasm [28]. The HSVs then replicate by three rounds of transcription and translation, such as the production of immediate early (IE) proteins that mainly regulate viral replication; the early proteins that synthesize and package



DNA; and the late proteins, most of which are part of the virions structure [1, 29]. In the course of this process, there is *de novo* synthesis and maturation of virions, and ultimately the progeny virus is transported to the plasma membrane for viral egress. The mature virions are released and are able to infect other nearby cells [1, 29, 30].

HSVs invade the body through the cells of the skin, the mucous membranes and the ocular surface [1, 29]. The primary infection of the epithelia causes a lytic infection and extensive cell death, the mechanism of which is complex, involving necrosis, apoptosis and autophagy/xenophagy [13-18, 31-37]. After the initial virus replication, progeny virions pass through the sensory nerve endings, are transported to sensory ganglia by retrograde axonal flow, and establish lifelong latency within the neuronal cells of the ganglia, brain stem, olfactory bulbs and temporal lobe [1, 29, 30]. During latent infection, viral nucleic acid is present in neurons, and the latency-associated transcripts are the only abundant viral RNAs expressed [1, 29, 30]. Following the establishment of a latent HSV infection in the nervous system, the inhibition of apoptosis predominates and maintains cell survival. However, systemic and local stressors can interrupt the latency and induce viral reactivation, leading to recrudescence infections [1, 29, 30, 38].

HSV-1 and HSV-2 have been identified as causative agents of various mild and even life-threatening diseases, including herpes simplex labialis, herpetic gingivostomatitis, genital herpes and keratitis [1, 29, 30, 39-43]. Primary herpetic oral, genital and ocular diseases are the most common manifestations of HSV infections [1, 29, 30, 40]. The majority of HSV-induced primary orofacial infections are subclinical and therefore unrecognized [40]. Herpetic gingivostomatitis, the most common orofacial manifestation of HSV infection, is preceded by a sensation of burning or paresthesia at the site of inoculation, cervical and submandibular lymphadenopathy, fever, malaise, myalgia, loss of appetite, dysphagia and headache. A few days later, numerous transient vesicles appear on the oral mucosa and rapidly rupture to cause painful, superficial ulcerations in and around the oral cavity [26, 29, 40]. Although both HSV-1 and HSV-2 may lead to primary oral infection, the majority of the oral herpetic infections are caused by HSV-1 [40]. Genital herpetic disease is most commonly caused by HSV-2, but the frequency of infections due to HSV-1 is currently increasing [40, 44, 45]. The appearance of genital herpetic lesions is often preceded by a prodrome of localized pain, tingling or a burning sensation. Within a few days of sexual contact, vesicles of varying sizes erupt on the genitals. These vesicles gradually rupture to form irregular ulcers and erosions which crust over and heal without scarring. Inguinal and femoral lymphadenopathy and cervicitis frequently accompany the primary infection. Complications of genital herpetic disease include aseptic meningitis, extragenital lesions and an autonomic dysfunction such as urinary

retention [40, 44]. In healthy individuals, primary infection has an excellent prognosis, with recovery expected within 10 to 14 days [40]. A wide variety of internal and external triggers may lead to reactivation of the virus. These include fever, immunosuppression, exposure to sunlight, psychological stress or local tissue trauma [40]. In most cases, the recurrent episodes are milder and shorter in duration [1, 29, 40]. Herpetic eye involvement may manifest clinically as blepharitis, conjunctivitis, keratitis, iridocyclitis and acute retinal necrosis [39, 46]. Primary herpetic ocular surface disease can develop directly via ‘front-door’ route infection by droplet spread, or via a ‘back-door’ route, which involves the indirect spread of HSV to the eye from a non-ocular site [39]. Serious ocular herpetic infection may affect all three corneal layers, leading to epithelial, stromal and endothelial keratitis [39, 47]. Epithelial keratitis, due to the direct cytopathic effect of HSV, can be characterized by the appearance of branching dendritiform or enlarged geographic ulcers [39, 46]. The underlying mechanisms that contribute to the development of stromal keratitis and endothelitis are complex, involving tissue damage triggered by HSV multiplication and indirect, immune-mediated events. HSV invasion of the corneal stroma induces an influx of innate immune cells [48-51]. The chronic immune-inflammatory reaction, together with the HSV-induced cytopathogenicity, can result in stromal scarring, thinning, neovascularization, severe iridocyclitis and an elevated intraocular pressure [39]. Most cases of corneal ulceration will eventually resolve, though these factors impair the corneal function and can lead to vision impairment [39, 46].

Although herpetic diseases are frequent and may lead to serious consequences, the molecular events implicated in the direct cytopathic effect of the HSVs remain unclear.

## **II. Vesicular stomatitis virus**

The *Vesicular stomatitis virus* (VSV) is a member of the *Vesiculovirus* genus of the *Rhabdoviridae* family. The virion is enveloped; bullet-shaped in structure and typically 100-400 nm long and 45–100 nm in diameter [52]. VSV comprises an 11-kilobase, negative-sense RNA genome that encodes for only five proteins, referred to as the nucleocapsid (N) protein, the phosphoprotein (P), the large (L) protein, the matrix (M) protein and the glycoprotein (G) [52]. The N, P and L proteins, in conjunction with specific host proteins, are responsible for both viral transcription and replication [52]. Protein G is a major antigen responsible for type specificity as it is a target for neutralizing antibody, and is additionally responsible for binding to host cells [52-57]. The M protein binds to the nucleocapsid core and exerts multiple functions. It has a crucial role in several processes, including virus assembly and budding. The M protein is required to shut off cellular mRNA synthesis and to

inhibit mRNA export. This protein is also an important mediator of apoptotic cellular responses triggered by VSV [52, 58-62].

In the course of its replication, VSV attaches to receptors on the surface of the host cell by the G protein [63, 64]. Thereafter, the virus penetrates the plasma membrane and uncoats to release the ribonucleoprotein particles [65]. After endocytosis, a drop in pH within the endosome causes membrane fusion, which releases the viral cores into the cytoplasm [65]. The L and P polymerase proteins, which are carried in with the virus, bind to the 3'-end of the genome and sequentially synthesize the five individual subgenomic mRNAs encoding N, P, M, G and L [52, 66]. The polymerases are also responsible for the replication of full-length viral genomes that are packaged into progeny virions [52, 66]. Newly synthesized N, P and L proteins associate in the cytoplasm and form ribonucleoprotein cores which bind to regions of the plasma membrane that are rich in both M and G proteins. The VSV particles are then formed and released by budding or through cellular lysis [52].

VSV has a broad host range and can cause epizootics among horses, cattle and swine. The rare VSV infections of humans are frequently asymptomatic or mild, characterized by fever, vesicular lesions in the mouth, lips and nose, pharyngitis, headache, retroorbital pain, nausea and vomiting [52, 67].

Interesting studies have demonstrated that VSV possesses powerful inherent oncolytic activity that can be exploited in the therapy of malignant tumors [7, 8, 66, 68-71]. The replication of VSV in immortalized cells is highly efficient, while in normal cells with a functional interferon (IFN) system it is restricted [72-74]. The finding that the IFN pathway is defective in the majority of transformed cell lines tested indicates that this signaling cascade is important in the regulation of cell growth, and it is dysregulated in cancer cells [75-79]. The double-stranded RNA-dependent protein kinase (PKR) is an IFN-inducible serine/threonine protein kinase that undergoes autophosphorylation following interaction with dsRNA [80-83]. Its most circumstantially characterized physiological substrate is the alpha subunit of eukaryotic initiation factor 2 (eIF2 $\alpha$ ) [80-83]. Phosphorylated eIF2 $\alpha$  effectively sequesters eIF2B, a rate-limiting component in the cell, and subsequently causes a dramatic inhibition in the initiation of translation. Thus, in normal cells, activation of PKR inhibits viral protein synthesis [80-83]. Tumors with a dysregulated IFN pathway could be considered defective in cellular defense responses and plausibly susceptible to VSV-mediated oncolysis [74]. A number of cell lines derived from lung, renal, colorectal, conjunctival, ovarian, breast, endometrial, prostate, central nervous system, melanoma and hematologic tumors have been demonstrated to be permissive to VSV [8, 9, 68-74, 84-87]. Nevertheless, the susceptibilities of other cell types have not yet been determined.

The mechanism of VSV-mediated oncolysis is linked to apoptotic mechanisms [73, 87, 88]. The M protein is known to be implicated in the apoptotic process triggered by VSV [58, 59]. The infection disrupts the mitochondrial transmembrane potential, leading to the death of infected cells [60]. It has also been established that VSV infection may induce a pro-apoptotic shift in the level of the Bcl-2 family member proteins [60, 89]. In certain experimental systems, the infected cells display decreased levels of some anti-apoptotic proteins, including Bcl-2 or Bcl-X<sub>L</sub>, and increased levels of some pro-apoptotic proteins, including p18 Bax [60, 89]. Furthermore, the over-expression of Bcl-2 or Bcl-X<sub>L</sub> confers significant protection against the pro-apoptotic effect of VSV [90].

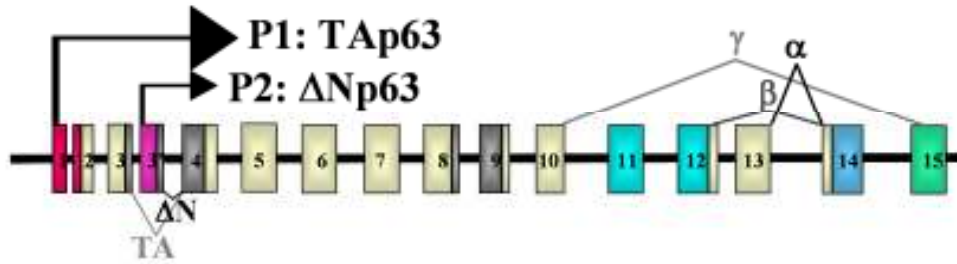
These noteworthy studies have demonstrated that VSV infection triggers both the intrinsic and extrinsic pathways of apoptosis in cancer cells. However, the underlying mechanisms involved in the oncolytic effects of this virus have not yet been fully defined.

### **III. The transcription factor p63 and its isoforms in epithelial cells**

The transcription factor p63 is a member of the p53 family that also includes p73 proteins [91]. The human *p63* gene resides on chromosome 3q27–29, and consists of 15 exons spread over about 270 kbp, with introns up to 100 kbp in length (Fig. 1) [91, 92]. There are different p63 protein isoforms, which can be expressed from two distinct promoters, one immediately preceding the first exon and the second one lying in the third intron (Fig. 1) [91-97]. Transcription from the first and second promoters gives rise to transactivating (TA) or amino terminally truncated ( $\Delta$ N) variations of p63, respectively [91-97]. The TA isoforms possess an N-terminal acidic transactivation domain, while the  $\Delta$ Np63 proteins lack this domain (Fig. 1) [91-97]. Both TA and  $\Delta$ N transcripts can undergo alternative splicing, leading to the formation of three C-terminal variants, denoted  $\alpha$ ,  $\beta$  and  $\gamma$ , which further increase the diversity of the p63 proteins (Fig. 1) [91-97].

All p63 isoforms contain a DNA-binding domain (DBD) and an oligomerization domain (OD). In addition, the  $\alpha$  isoforms contain a sterile alpha motif (SAM) and a transactivation inhibitory domain (TID). The former is a protein-protein interaction domain, while the latter is an inhibitory domain that blocks transactivation by masking a few residues on the N-terminal of the TA domain, and in this way could be responsible for oligomerization between different p63 isoforms [93]. The  $\beta$  variants lack exon 13 and consequently the SAM and the TID domains (Fig. 1). The  $\gamma$  isoforms lack the C-terminal exons 11, 12, 13 and 14, but incorporate an additional sequence of exon 15 (Fig. 1) [98].

### A. Human p63 gene structure



### B. Human p63 protein isoforms



**Fig. 1.** (A) Gene architecture of human p63. The alternative promoters and splicing events used to generate the various p63 isoforms are indicated. (B) Domain structure of the various p63 proteins. The transcription activation domain (TAD), DNA binding domain (DBD), oligomerization domain (OD), sterile  $\alpha$  motif (SAM) and transinhibitor domain (TID) are depicted. The molecular size of each isoform is indicated on the right. (Not drawn to scale; adapted from [91-97] .) aa, amino acid

TAp63 and  $\Delta$ Np63 isoforms have the ability to regulate a number of genes and possess opposing regulatory effects [91-111]. As sequence-specific transcription factors, the TAp63 isoforms bind p53-responsive elements (p53-RE), stimulate the expression of p53 target genes, such as the *bax* gene, and exert biological functions that partially overlap with those of p53. The TAp63 isoforms also interact with the p63 DNA consensus motif, which is not recognized by p53. Thus, a unique set of genes, which contains p63-RE, but lacks p53-RE in its regulatory region, exhibits specific responsiveness to p63 [91, 93]. The TAp63 proteins have been reported to induce growth arrest and apoptosis in a manner consistent with their transactivation capabilities [92, 99-101, 104-108]. The various TA isoforms display widely differing transcriptional efficiencies; proteins with  $\beta$  and  $\gamma$  C-termini exhibit higher transactivation potentials than that of TAp63 $\alpha$ , which contains TID. In contrast, the  $\Delta$ Np63 isoforms may exert dominant-negative activities by antagonizing the target gene induction

triggered by TAp63 isoforms and p53 [99, 105, 107]. Moreover, these isoforms can actively repress or activate transcription, possibly in consequence of the presence of two cryptic transactivation domains [111, 112]. The  $\Delta$ Np63 isoforms have been shown to inhibit apoptosis and exert oncogenic properties [91, 94, 99, 100, 103, 108].

The six p63 isoforms regulate a wide array of cellular functions, including cell cycle progression, proliferation, adhesion, senescence and apoptosis; thereby, they play important roles in embryonic development, tumor progression and certain physiological processes and pathological conditions that affect the epithelial tissues [91-108]. Noteworthy studies have clearly demonstrated that p63 is instrumental in the development and maintenance of epithelial tissues [91-101]. Its role has been elucidated in large part through the analysis of p63-deficient mice, which display developmental abnormalities including the complete lack of limbs, stratified epithelia and derivative structures such as skin, breast, prostate and hair follicles [95, 96]. A range of human syndromes characterized by ectodermal dysplasia have been linked to a diversity of heterozygous p63 mutations [113]. Although p63 does not conform to Knudson's two-hit hypothesis, the dysregulated expression of p63 has been shown to contribute to the pathogenesis of cancers [97, 114]. Previous studies have also demonstrated that p63 isoforms are involved in the control of the epithelial cell fate and in the regulation of the differentiation program of the skin and the eye [91, 93-97].

Within the mature epidermis,  $\Delta$ Np63 $\alpha$  is the predominant isoform, expressed in high levels in the basal layer of the skin [91-94].  $\Delta$ Np63 $\alpha$  is indispensable for maintenance of the viability and proliferative potential of basal keratinocytes, and it is also essential to prevent the premature entry of cells into the differentiation program. The expression of  $\Delta$ Np63 $\alpha$  is downregulated as keratinocytes commit to the process of differentiation, while the TAp63 isoforms are required to achieve terminal differentiation [91-94].

Within the ocular surface epithelia, no expression of the TAp63 isoforms can be detected. In contrast,  $\Delta$ Np63 $\alpha$  is detected in high levels within the basal to intermediate layers of the limbal and conjunctival epithelia [115]. This p63 isoform seems to be indispensable for the viability and proliferative potential of the ocular surface epithelial stem cell population [106-120]. Neither  $\Delta$ Np63 $\beta$  nor  $\Delta$ Np63 $\gamma$  has been shown to be present in substantial amounts within the conjunctiva, the limbus or the cornea [115]. However, following injury, dramatic increases are detected in the low-level constitutive expression of these p63 isoforms within the regenerating corneal tissue [120].

#### IV. The Bcl-2-associated X protein (Bax) and its apoptotic regulatory functions

The Bcl-2-associated X protein, or Bax, is a product of the *Bcl-2* gene family. *Bcl-2* is an oncogene, which is frequently linked in follicular lymphoma to an immunoglobulin locus by the chromosome translocation t(14:18) [121]. It was the first example of an oncogene that inhibits cell death rather than promotes proliferation. When homologs of Bcl-2 were identified, it became apparent that these proteins can be defined by the presence of conserved sequence motifs known as Bcl-2 homology domains (BH1 to BH4) [122]. In mammals, up to 30 relatives have been described, some of which belong in an anti-apoptotic group and others in a pro-apoptotic group [123]. Besides Bcl-2 itself, there are several other anti-apoptotic proteins (Bcl-w, Mcl-1, Bcl-X<sub>L</sub> and A1/Bfl-1), which all possess the domains BH1, BH2, BH3 and BH4. The pro-apoptotic group of the Bcl-2 family can be divided into two subgroups. The multi-domain pro-apoptotic subgroup consists of Bax, Bak and Bok, which all possess the domains BH1, BH2 and BH3, whereas the BH3-only proteins (Bid, Bim, Bik, Bad, Bmf, Hrk, Noxa, Puma, Blk, BNIP3 and Spike) have only the short BH3 motif, an interaction domain that is both necessary and sufficient for their pro-apoptotic effect (Fig. 2) [122, 123, 124].

The *bax* gene encodes multiple splice variants [125]. The alternatively splicing patterns of the *bax* gene are highly complex. Nine Bax isoforms have been identified thus far, including Bax- $\alpha$ , Bax- $\beta$ , Bax- $\gamma$ , Bax- $\delta$ , Bax- $\epsilon$ , Bax- $\sigma$ , Bax- $\zeta$ , Bax- $\omega$  and Bax- $\psi$  [126]. The mRNA for Bax- $\alpha$  encodes a 21-kDa protein, while the mRNA for Bax- $\beta$  encodes a 24-kDa protein (Fig. 2) [126]. It is well documented that Bax- $\alpha$  is a central component of apoptosis induction [111, 124, 127]. Bax- $\alpha$  can be found as a cytosolic monomer in viable cells. During apoptosis, Bax- $\alpha$  changes its conformation, integrates into the outer mitochondrial membrane and oligomerizes [122, 123]. Although the mechanism is controversial, Bax- $\alpha$  and Bak oligomers are believed to provoke or contribute to the permeabilization of the outer mitochondrial membrane, either by forming channels themselves or by interacting with components of the permeability transition pore [122, 123]. This results in the release of cytochrome *c* and other pro-apoptotic factors from the mitochondria, leading to the activation of caspases and apoptosis [128]. Recent studies have clarified the function of Bax- $\beta$  [126, 129]. The Bax- $\beta$  protein is expressed constitutively in several human cell types, and its level is controlled by proteasomal degradation. Similarly to Bax- $\alpha$ , Bax- $\beta$  has the capability to trigger apoptosis via the mitochondrial pathway. Moreover, Bax- $\beta$  facilitates Bax- $\alpha$  activation [126]. In this way, both proteins play important roles in the intrinsic pathway of apoptosis. A few data suggest that most alternatively spliced Bax variants are active as pro-apoptotic

proteins, but the functions of the Bax- $\gamma$ , Bax- $\delta$ , Bax- $\epsilon$ , Bax- $\sigma$ , Bax- $\zeta$ , Bax- $\omega$  and Bax- $\psi$  isoforms are not yet fully known [126]. Other interesting studies have revealed that proteolytic processing of Bax- $\alpha$  may further increase the diversity of the Bax isoforms. Cleavage of the Bax- $\alpha$  protein at a late stage of apoptosis by cellular enzymes has been shown to remove the first 33 amino acids of the N-terminus, resulting in transition from the p21 Bax to the p18 Bax form [130, 131]. The accumulation of the p18 Bax variant is an important event in the amplification and acceleration of the apoptotic process [131].

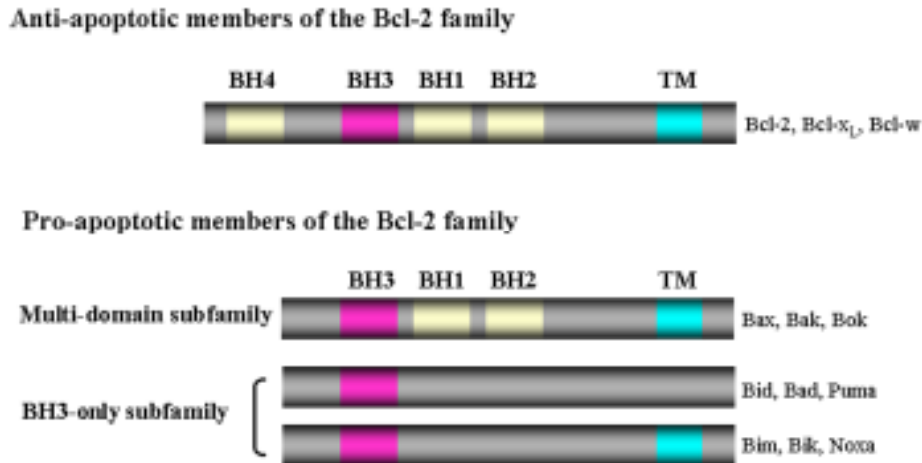


**Fig. 2.** Structure of the various Bcl-2 family member proteins. The BH1, BH2 and BH3 domains of the proteins are indicated. (Not drawn to scale; adapted from [125-127].)

The epithelia of the skin and eye may be exposed to harmful environmental stimuli, such as ultraviolet light exposure, and may also function as entry sites for a wide array of human pathogenic microorganisms. By disturbing the delicate balance between the pro-survival  $\Delta N$  and the pro-apoptotic TA isoforms, stress signals that alter the expression of p63 may cause profound alterations in the viability of the keratinocytes and ocular cells. However, the effects of microorganisms on the expression patterns of p63 and Bax have not yet been elucidated.

## AIMS

### I. A. Investigation of the p63, p73 and Bax expression patterns in HSV-infected primary keratinocytes and HaCaT cells

In an effort to gain more insight into the pathogenic mechanisms of skin infections caused by HSV-1 and HSV-2, we set out to investigate the effects of these viruses on the levels of p63, p73 and Bax expression. Our aims were as follows:

- a) To investigate the susceptibilities of the HaCaT keratinocyte cell line and primary keratinocytes to HSV-1 and HSV-2.



- b) To investigate the role of apoptosis in the cell demise triggered by HSV-1 and HSV-2.
- c) To analyze the expression levels of p63, p73 and Bax in HSV-1- or HSV-2-infected HaCaT keratinocytes.

### **I. B. Investigation of the p63 and Bax expression patterns in HSV-1-infected SIRC corneal cell line**

In an effort to gain more insight into the pathogenic mechanism of herpetic ocular surface disease, we set out to investigate the effects of HSV-1 on the levels of p63 and Bax expression. Our aims were as follows:

- a) To investigate the susceptibility of the Staatens Serum Institute Rabbit Cornea cell line (SIRC) to HSV-1.
- b) To investigate the role of apoptosis in the cell demise triggered by HSV-1.
- c) To analyze the expression levels of p63 and Bax in HSV-1-infected SIRC cells.

### **II. Investigation of the p63 and Bax expression patterns in VSV-infected HaCaT keratinocyte cell line**

In an effort to evaluate the potential oncolytic activity of VSV in epithelial-derived skin cancers, we set out to investigate the cytopathogenicity of this virus in the immortalized HaCaT keratinocyte cell line. Our aims were as follows:

- a) To investigate the susceptibility of the HaCaT cell line to VSV.
- b) To investigate the role of apoptosis in the cell demise triggered by VSV.
- c) To analyze the expression levels of p63 and Bax in VSV-infected HaCaT cells.

## **MATERIALS AND METHODS**

### ***Cell cultures***

**HaCaT cells:** The HaCaT cell line, kindly provided by Dr. N. E. Fusenig (Heidelberg, Germany), originally derived from the distant periphery of a melanoma located on the upper half of the back of a 62-year-old male patient. The line is clonal in origin as indicated by specific and stable cytogenetic markers, has a transformed phenotype *in vitro* but is not tumorigenic, and is noninvasive *in vivo*, however it expresses mutated p53 (p53<sup>mt</sup>) [132]. The cells were grown at 37 °C in a 5% CO<sub>2</sub> atmosphere in Dulbecco's modified Eagle's minimal essential medium (Sigma Chemical Co., St. Louis, MO, USA) supplemented with 10% fetal calf serum (Gibco/BRL, Grand Island, NY, USA).

**Primary keratinocytes:** The normal human primary keratinocytes, kindly provided by Prof. Dr. Lajos Kemény (Department of Dermatology and Allergology, University of Szeged,

Hungary), were cultured at 37 °C in a 5% CO<sub>2</sub> atmosphere in keratinocyte growth medium (Gibco/BRL).

**SIRC cell line:** The SIRC cell line was obtained from the European Collection of Cell Cultures [(ECACC) (Health Protection Agency Culture Collections, Porton Down, UK)]. Cells were grown in Dulbecco's modified Eagle's minimal essential medium (Sigma) supplemented with 10% fetal bovine serum (Gibco/BRL) at 37 °C in a 5% CO<sub>2</sub> atmosphere.

### *Viruses*

**Herpes simplex viruses:** The KOS strain of HSV-1 and the wild-type HSV-2 were propagated at an MOI of 0.001 PFU per cell in Vero cell cultures for 3 days at 37 °C. The culture fluids of HSV-1- or HSV-2-infected Vero cells were harvested, stored at -70 °C, and used as the infecting stock of the virus.

**Vesicular stomatitis virus:** The Indiana strain of VSV was propagated at a multiplicity of infection (MOI) of 0.001 plaque forming unit (PFU) per cell in L929 cell cultures for 3 days at 37 °C. The culture fluid of VSV-infected L929 cells was harvested, stored at -70 °C, and used as the infecting stock of the virus.

### *Methods used to detect virus replication and host cell viability*

**Indirect immunofluorescence assay:** Cytospin cell preparations were fixed in methanol-acetone (1:1) for 15 minutes (min) at -20 °C. Slides were incubated with a 1:500 dilution of VSV G protein-specific monoclonal antibody (MAb) (Sigma) or 1:200 dilution of HSV gD-specific MAb (Santa Cruz Biotechnology Inc., Cambridge, MA, USA) for 1 hour (h) at 37 °C. After washing with phosphate-buffered saline (PBS), the samples were reacted with fluorescein isothiocyanate (FITC)-conjugated anti-mouse antibody (1:160) (Sigma) and incubated for 1 h at 37 °C. After washing with PBS, the slides were visualized by confocal microscopy. The ratio of positive to negative cells was determined after counting 1000 cells in random fields.

**Quantification of virus replication by plaque titration:** Virus plaque assays were performed on confluent monolayers of Vero cells inoculated with HSV or VSV for 1 h at 37 °C and overlaid with 0.5% agarose (FMC, Rockland, ME) in phenol red-free Eagle's minimum essential medium supplemented with 7.5% fetal bovine serum and 2 mM L-glutamine. After 2 days of culturing at 37 °C, a second agarose overlay containing 0.005% neutral red was added. Plaque titers were determined at 3 days after infection.

**Quantification of cell viability by MTT assay:** The viability of virus-infected cells was measured with the colorimetric MTT [3-(4,5-dimethylthiazol-2-yl)2,5-diphenyltetrazolium

bromide] assay Tox-1 kit (Sigma). In this assay, the cells were seeded in 96-well plates at a density of  $1 \times 10^4$ /well. The cultures were infected with HSV or VSV at different MOIs. At 24 or 48 hours postinfection (hpi) at 37 °C, 10 µl MTT reagent (5 mg/ml) was added to each well. After 2 h incubation, MTT solvent containing 0.1 M HCl and isopropanol was added for 15 h. Absorbance was measured at 545 and 630 nm. The ratio of living cells was calculated via the following formula: percentage viability = [(absorbance of infected cells – blank) / (absorbance of corresponding mock-infected control cells – blank)] x 100.

**Inhibition of viral DNA replication:** To inhibit the DNA replication of HSV-1 and HSV-2, 9-[(2-Hydroxyethoxy)methyl]guanine [(ACG) (Sigma)] was used at various concentrations when indicated.

### *Methods used to detect apoptosis*

**Quantification of apoptosis by enzyme-linked immunosorbent assay (ELISA):** The cells were washed in PBS and the cell pellet was processed in a cell death detection ELISA kit (Roche Diagnostics GmbH, Penzberg, Germany) based on the measurement of histones complexed with mono- and oligonucleosome fragments formed during cell death. For this assay, the cells were incubated in lysis buffer for 30 min and centrifuged at 12,000 rpm for 10 min. The supernatants were transferred into a streptavidin-coated microplate and incubated with biotin-conjugated anti-histone and peroxidase-conjugated anti-DNA monoclonal antibodies for 2 h. After washing, substrate solution 2,2'-azino-bis(3-ethylbenzthiazoline-6-sulphonic acid) (ABTS) was added to each well for 15 min. Absorbance was measured at 405 and 490 nm. The specific enrichment of mono- and oligonucleosomes was calculated as the enrichment factor (EF) = absorbance of infected cells/absorbance of corresponding non-infected control cells.

**Quantification of apoptosis by annexin V staining:** The cells were stained with FITC-labeled annexin V and propidium iodide (PI) (Bender MedSystems Inc., Burlingame, CA, USA) according to the manufacturer's instructions. The fluorescence intensities of annexin-FITC and PI were determined with a FACStar Plus flow cytometer (BD Biosciences, San Diego, CA, USA) by using the WinMDI software. The percentages of apoptotic cells were calculated by sorting the cells that were positive only for annexin V (early apoptotic stage) or positive for both annexin V and PI (late apoptotic and necrotic stages).

### *Methods used to identify proteins*

**Western blot assays:** Cells ( $1 \times 10^7$ ) were homogenized in ice-cold lysis buffer containing 150 mM NaCl, 10 mM Tris·HCl, pH 7.6, 5 mM EDTA, 1% (v/v) Nonidet P-40, 0.1% SDS,

1% sodium deoxycholate and protease inhibitor cocktail (Sigma), and the mixture was then centrifuged at 10,000 g for 10 min to remove cell debris. Protein concentrations of cell lysates were determined by using the Bio-Rad protein assay (Bio-Rad, Hercules, CA, USA). Supernatants were mixed with Laemmli's sample buffer and boiled for 3 min. Aliquots of the supernatants, containing 50 µg of total protein to detect HSV gD, VSV G protein, p53, p63, p73, Bax and β-actin, were resolved by SDS-polyacrylamide gel electrophoresis (PAGE) and electrotransferred onto nitrocellulose filters (Amersham, Buckinghamshire, UK). Preblocked blots were reacted with specific antibodies to VSV G protein (Sigma), HSV gD (Sigma), p63 (clone 4A4) detecting all of the various p63 isoforms (Santa Cruz), p40 detecting the ΔNp63 isoforms (Merck KGaA, Darmstadt, Germany), p53 (Serotec Inc. Raleigh, NC), p73 (clone H-79) detecting all of the various p73 isoforms (Santa Cruz), β-actin (Sigma), and Bax (PharMingen, SanDiego, CA) for 4 h in PBS containing 0.05% (v/v) Tween 20, 1% (w/v) dried non-fat milk (Difco Laboratories, Detroit, MI) and 1% (w/v) BSA (fraction V; Sigma). Blots were then incubated for 2 h with species-specific secondary antibodies coupled to peroxidase [peroxidase-conjugated anti-mouse antibody (DakoCytomation, Carpinteria, CA, USA), or peroxidase-conjugated anti-rabbit antibody (DakoCytomation)]. Filters were washed five times in PBS–Tween for 5 min after each step and were developed by using a chemiluminescence detection system (Amersham). The autoradiographs were scanned with a GS-800 densitometer (Bio-Rad), and the relative band intensities were quantified by use of the ImageQuant software (Amersham).

**Gene silencing by small interfering RNA (siRNA):** Chemically synthesized siRNA targeting TAp63 (Silencer siRNA 4798) and non-silencing control siRNA (Silencer negative control #2 siRNA 4613) were obtained from Ambion Inc. (Austin, TX, USA). Transient transfections were performed by using the siPORT amine reagent (Ambion) according to the manufacturer's protocol, with a final siRNA concentration of 50 nM. The transfected HaCaT cells were incubated at 37 °C in a humidified atmosphere of 5% CO<sub>2</sub> for 48 h. The effect of silencing was analyzed at the protein level by Western blot assay.

### ***Statistical analysis***

All values are expressed as means ± standard deviation (SD). Student's unpaired *t* test was used for comparisons and *P* values < 0.05 were considered statistically significant. The one-way ANOVA test with the Bonferroni post-test was used for pairwise multiple comparisons, and *P* values < 0.05 were considered statistically significant.

## RESULTS

### *I. A. The effects of HSV infection on the expression patterns of p63, p73 and Bax in HaCaT cells and primary keratinocytes*

#### **I. A. 1. The HaCaT cell line is permissive for HSV-1 replication**

The HaCaT cells were infected with the KOS strain of HSV-1 at various multiplicities and maintained for different periods of time. The production of progeny virus was determined by plaque titration of the culture supernatants taken from HaCaT cells at 6, 12, 24 or 48 hpi.

Depending on the infectious dose, the level of HSV-1 production varied between  $<5 \times 10^2$  and  $1 \times 10^4$  PFU/ml at 6 hpi (Table 1). The virus titers thereafter increased, and ranged from  $6 \times 10^6$  and  $3.3 \times 10^8$  PFU/ml at 48 h after inoculation. Accordingly, the maximum yield at 0.001, 0.01, 0.1, 1 and 10 MOI corresponded to 30, 550, 600, 1650 and 1500 PFU/cell, respectively. These data demonstrate that HSV-1 replicates efficiently in the HaCaT keratinocyte cell line.

Table 1. Viral titers in HSV-1-infected HaCaT cells

MOI	Titer of HSV-1 (PFU/ml)			
	6 h	12 h	24 h	48 h
<b>0.001</b>	$<5 \times 10^2$	$<5 \times 10^2$	$1.7 \times 10^4$	$6 \times 10^6$
<b>0.01</b>	$<5 \times 10^2$	$<5 \times 10^2$	$1.6 \times 10^6$	$1.1 \times 10^8$
<b>0.1</b>	$5 \times 10^2$	$1 \times 10^3$	$8 \times 10^6$	$1.2 \times 10^8$
<b>1.0</b>	$2 \times 10^3$	$3.5 \times 10^3$	$1.7 \times 10^8$	$3.3 \times 10^8$
<b>10</b>	$1 \times 10^4$	$4.7 \times 10^5$	$1.5 \times 10^8$	$3 \times 10^8$

#### **I. A. 2. HSV-1 and HSV-2 trigger cell death in the HaCaT keratinocyte cell line**

The cytopathogenicity of HSV-1 and HSV-2 was determined by the MTT assay. HSV-1-infected cells displayed decreased viability at 24 hpi; the proportions of dead cells were 9, 28, 38 and 50% at MOIs of 0.01, 0.1, 1 and 10, respectively (Fig. 3A). HSV-2-infected cells likewise exhibited decreased viability; at 24 h after inoculation the proportions of dead cells were 9, 21, 42 and 50% at MOIs of 0.01, 0.1, 1 and 10, respectively (Fig. 3A).

To examine the ability of HSV-1 and HSV-2 to induce apoptosis in HaCaT cells, the extent of apoptosis was measured by annexin V binding assay at 24 hpi. The proportions of annexin V-single-positive (early apoptotic) and double-positive (early apoptotic and necrotic) cells in cultures infected with HSV-1 at an MOI of 10 were 21 and 16%, respectively (Fig. 3B). In contrast, the proportions of annexin V-single-positive and double-positive cells in cultures infected with HSV-2 at an MOI of 10 were 12 and 25%, respectively (Fig. 3B).

These results indicate that HSV-1 and HSV-2 trigger different types of cell death in HaCaT cultures.

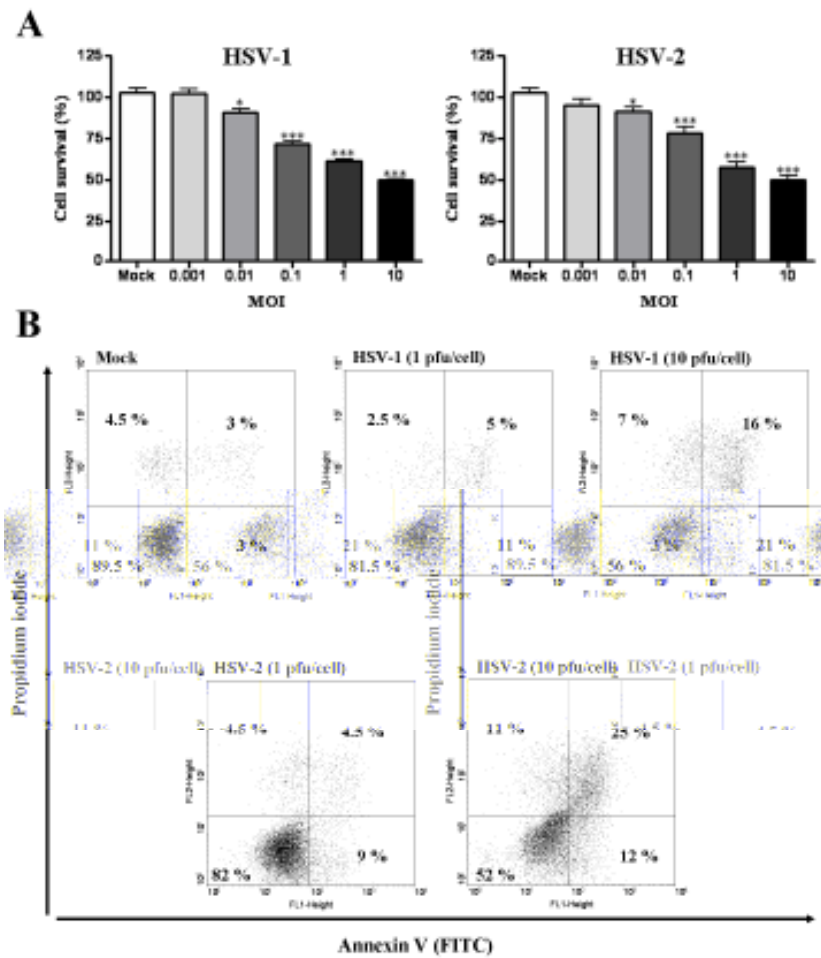


**Fig. 3.** HSV-1 and HSV-2 induce cell death in the HaCaT keratinocyte cell line. Cellular viability was measured by the MTT assay at 24 hpi (A). Apoptosis was measured by annexin V staining (B). \* $P < 0.05$ ; \*\*\* $P < 0.001$ .

### I. A. 3. HSV-1 and HSV-2 alter the levels of Bax, p63 and p73 in a serotype-specific manner

To determine whether HSV-1 and HSV-2 can alter the expressions of Bax, p63 and p73 in the HaCat cell line, the steady-state levels of these proteins were determined by Western blot analysis. Experiments to investigate the kinetics of HSV-1 replication revealed the presence of gD in cultures infected with HSV-1 as early as 6 hpi (Fig.4; lane 18). The level of gD thereafter increased, and its expression was highly upregulated in every culture infected with HSV-1 at 48 h after inoculation (Fig. 4; lanes 32-36).

Mock-infected HaCaT cells displayed the endogenous expression of Bax- $\alpha$ , which remained constant during the 48 h of culturing (Fig. 4; lanes 1, 7, 13, 19, 25 and 31). Interestingly, the analysis revealed the presence of a Bax isoform corresponding to Bax- $\beta$  in HSV-1-infected cultures as early as 6 hpi (Fig. 4; lane 18). The level of Bax- $\beta$  thereafter

increased, and its expression was highly upregulated in every culture infected with HSV-1 by 48 hpi (Fig. 4; lanes 32-36).

The expression pattern of p63 was determined by using an antibody preparation, which recognizes all of the various p63 isoforms. The analysis demonstrated that the predominant isoform in the HaCaT cell line is a p63 protein migrating near 68 kDa. HSV-1 triggered an impressive reduction in the level of this 68 kDa p63 isoform. The HSV-1-infected cells exhibited decreased levels of this protein as early as 12 hpi (Fig. 4; lanes 23-24). The expression of the 68 kDa p63 isoform was downregulated in cells infected at MOIs of 0.1, 1 and 10 at 48 h after inoculation (Fig. 4; lanes 32-36). Interestingly, a p63 isoform migrating between 51 and 62 kDa was also detected in HSV-1-infected cells as early as 6 hpi (Fig. 4; lane 18). The level of the 51-62 kDa p63 isoform thereafter increased, and the expression of this protein was highly upregulated in every culture infected with HSV-1 by 48 hpi (Fig. 4; lanes 32-36).

Given the high number of possible, functionally diverse p63 isoforms, an exact assignment of the isoforms to the proteins detected by Western blot analysis through use of the pan-p63-specific antibody is difficult. Thus, to identify the p63 isoforms, the steady-state levels of these proteins were also determined by Western blot analysis, using a polyclonal antiserum which reacts only with the  $\Delta N$  forms. The  $\Delta N$ p63-specific antibody preparation detected the 68 kDa p63 isoform, but failed to recognize the 51-62 kDa p63 isoform in HSV-1-infected cultures. This result indicates that the 68 kDa isoform belongs in the  $\Delta N$  subclass and might be identical with  $\Delta N$ p63 $\alpha$ , while the 51-62 kDa isoform is a member of the TA subclass and corresponds to TAp63 $\gamma$ . Furthermore, these experiments confirmed that the level of  $\Delta N$ p63 $\alpha$  was decreased, while the expression of TAp63 $\gamma$  was highly increased following HSV-1 infection (Fig. 4; lanes 1-36).

The expression pattern of p73 was determined by using an antibody preparation which recognizes all of the various p73 isoforms. Mock-infected HaCaT cells expressed two p73 isoforms, migrating near 50 and 44.5 kDa, the levels of which remained constant during the 48 h of culturing (Fig. 4; lanes 1, 7, 13, 19, 25 and 31). The HSV-1-infected cells exhibited a decreased level of the 50 kDa p73 isoform at 24 h after virus inoculation (Fig. 4; lanes 26-30). In every infected culture, the expression of this protein was likewise downregulated by 48 hpi (Fig. 4; lanes 32-36). The HSV-1-infected cells displayed an increased level of the 44.5 kDa p73 isoform at 24 hpi (Fig. 4; lanes 26-30). Similarly, the level of this protein was upregulated by 48 hpi in cultures infected with HSV-1 at MOIs of 0.01, 0.1, 1 and 10 (Fig. 4; lanes 33-36).

Experiments to investigate the replication of HSV-2 revealed the presence of gD in cultures infected with HSV-2 at 24 hpi (Fig. 4; lanes 40-42). The levels of the 50 and 44.5 kDa p73 isoforms and  $\Delta$ Np63 $\alpha$  were decreased, Bax- $\alpha$  and TAp63 $\gamma$  remained unaffected, while the expression of Bax- $\beta$  was slightly increased at 24 h after inoculation in HSV-2-infected HaCaT cells (Fig. 4; lanes 38-42). These findings suggest that HSV-1 and HSV-2 alter the levels p63, p73 and Bax in a type-specific manner in HaCaT epithelial cell cultures.

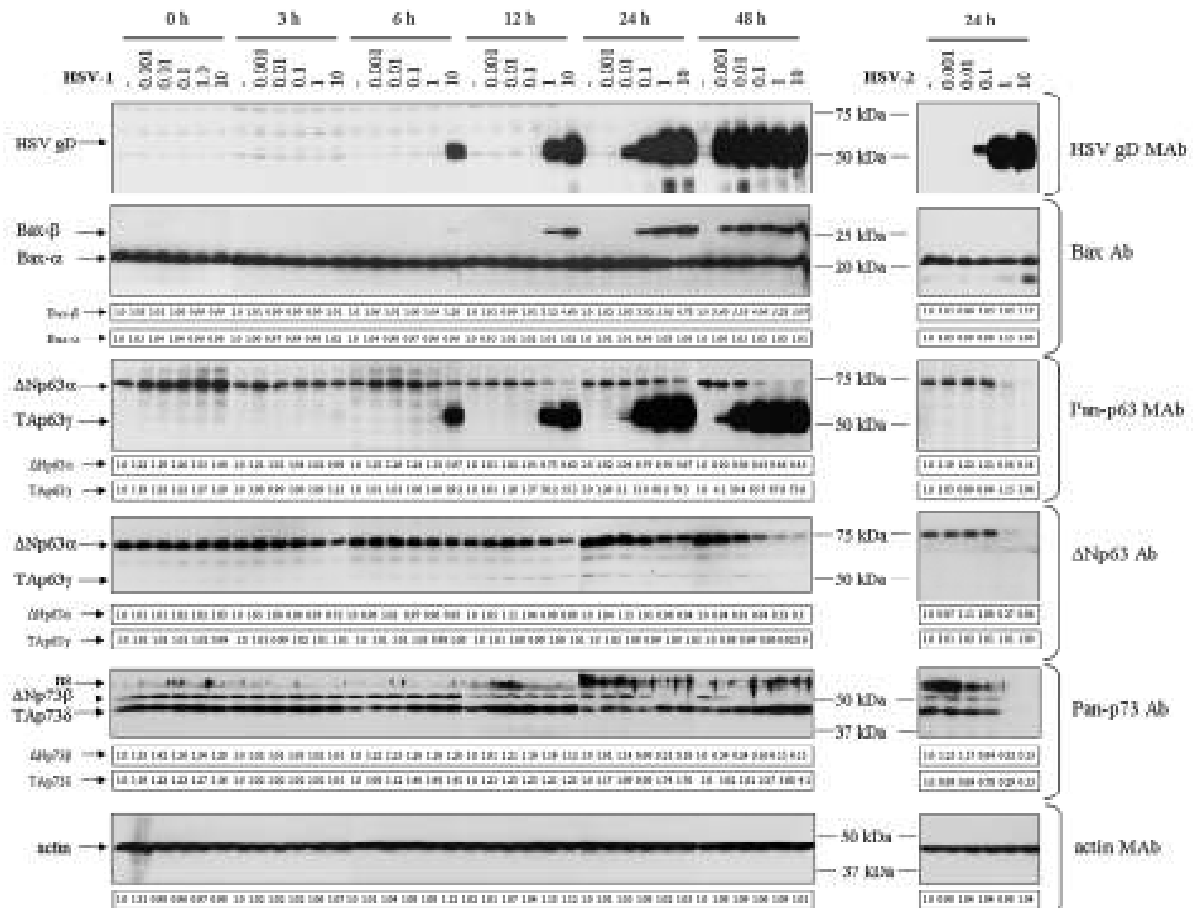


**Fig. 4.** HSV-1 and HSV-2 differentially modulate the levels of Bax, p63 and p73 in the HaCaT keratinocyte cell line. The steady-state levels of proteins were analyzed by Western blot assay. To quantify protein levels in HSV-infected cells, band intensities were determined by densitometric analysis with the ImageQuant software. The numbers indicate the relative quantities of each band, normalized to the control cells at each time point.

#### I. A. 4. HSV-1 alters the levels of Bax and p63 in primary keratinocytes

To determine whether HSV-1 can dysregulate the expressions of Bax and p63 in primary keratinocytes, the steady-state levels of these proteins were determined by Western blot analysis. Primary keratinocytes were infected at an MOI of 1, and the kinetics of HSV-1 replication was investigated. The experiments revealed the presence of gD in cultures infected



with HSV-1 as early as 6 hpi, and its level was highly increased at 12 and 24 h after inoculation (Fig. 5; lanes 6, 8, 10).

The mock-infected cells displayed the endogenous expression of the wild-type p53 protein (p53<sup>wt</sup>),  $\Delta$ Np63 $\alpha$  and Bax- $\alpha$  (Fig. 5; lanes 1, 3, 5, 7, 9). The level of  $\Delta$ Np63 $\alpha$  was decreased, p53<sup>wt</sup> and Bax- $\alpha$  remained unaffected, while the expressions of the Bax- $\beta$  and TAp63 $\gamma$  were highly increased by 12 hpi in HSV-1-infected primary keratinocytes (Fig. 5; lane 8). These data indicate that HSV-1 alters the levels of Bax and p63 in primary keratinocytes.

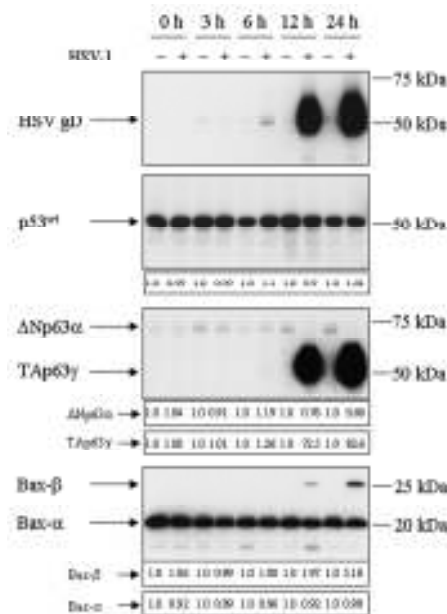


**Fig. 5.** HSV-1 alters the levels of Bax and p63 in primary keratinocytes. The steady-state levels of proteins were analyzed by Western blot assay. To quantify protein levels in HSV-1-infected cells, band intensities were determined by densitometric analysis with the ImageQuant software. The numbers indicate the relative quantities of each band, normalized to the control cells at each time point.

#### I. A. 5. HSV-1-mediated TAp63 $\gamma$ expression requires viral DNA replication

To investigate the basis of the HSV-1-induced accumulation of TAp63 $\gamma$ , HaCaT cells were infected in the presence or absence of the viral DNA replication inhibitor ACG. The cells were analyzed for the presence of p63 and Bax by Western blot analysis.

The lack of the late protein gD in samples treated with 100, 50 or 10  $\mu$ g/ml ACG indicated that the drug treatment inhibited viral DNA replication efficiently (Fig. 6; lanes 2, 3, 4). In HSV-1-infected cells treated with 100, 50 or 10  $\mu$ g/ml ACG, the levels of Bax- $\beta$  and TAp63 $\gamma$  were decreased, Bax- $\alpha$  remained constant, while the expression of  $\Delta$ Np63 $\alpha$  was increased, as compared with HSV-1-infected cultures maintained in the absence of ACG

(Fig. 6; lanes 2, 3, 4 and 1). These findings demonstrate that the HSV-1-mediated TAp63 $\gamma$  expression requires viral DNA replication.

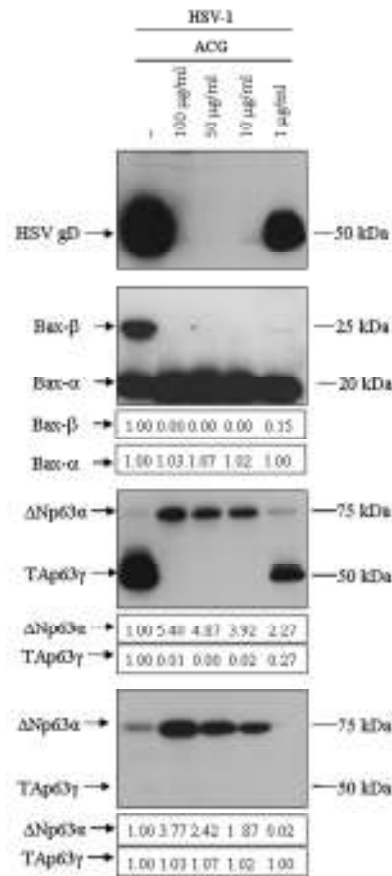


**Fig. 6.** HSV-1-mediated TAp63 $\gamma$  expression requires viral DNA replication. HaCaT cells were infected with the KOS strain of HSV-1 at an MOI of 1 and maintained for 24 h in the presence or in the absence of ACG. The steady-state levels of Bax and p63 isoforms were analyzed by Western blot assay. To quantify protein levels in HSV-1-infected cells, band intensities were determined by densitometric analysis with the ImageQuant software. The numbers indicate the relative quantities of each band, normalized to the control cells at each time point.

#### I. A. 6. Knockdown of HSV-1-induced TAp63 expression increases the viability of infected HaCaT cells

To evaluate the biological effects of the accumulation of TAp63 $\gamma$  in HSV-1-infected cells, siRNA technology was used. The delivery of TAp63-specific siRNA resulted in an 85% reduction in HSV-1-induced TAp63 $\gamma$  expression as compared with cultures treated with a negative control siRNA preparation (Fig. 7A). In the presence of the TAp63-specific siRNA, the viability of HSV-1-infected cells was increased by about 15% at 24 hpi (Fig. 7B). These results confirm that the 51-62 kDa p63 isoform corresponds to the TA subclass, and suggest that TAp63 $\gamma$  may play some role in the cytopathogenicity of HSV-1.

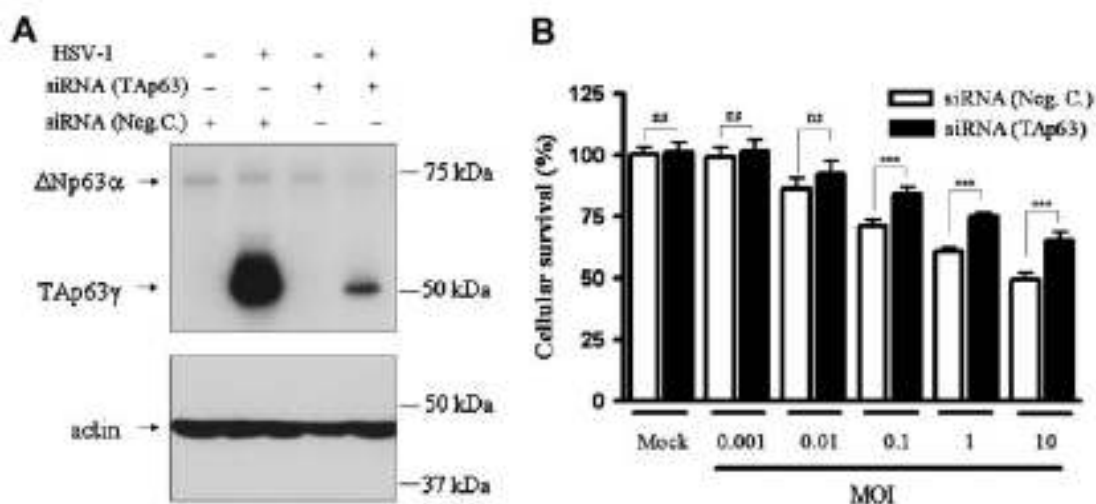


**Fig. 7.** Knockdown of HSV-1-induced TAp63 expression increases the viability of infected HaCaT cells. The expression of TAp63 was knocked down by the delivery of TAp63-specific siRNA. HaCaT cells were infected with the KOS strain of HSV-1 at an MOI of 5 and maintained for 24 h. Mock-infected cultures incubated in parallel were left untreated. Total protein was isolated and p63 isoforms were detected by Western blot assay (A). The cellular viability was measured by using the MTT assay (B). \*\*\* $P < 0.001$ . +: present; -: absent.

### ***I. B. The effects of HSV infection on the expression patterns of p63 and Bax in SIRC cells***

#### **I. B. 1. HSV-1-infected SIRC cells exhibit gD expression and increased apoptotic rates**

The SIRC cell line was infected with the KOS strain of HSV-1 at various multiplicities and maintained for different periods of time. Indirect immunofluorescence assays to evaluate HSV-1 replication revealed positive staining for gD at 48 hpi in  $\geq 99\%$  of SIRC cells infected at an MOI of 1 (Fig. 8).

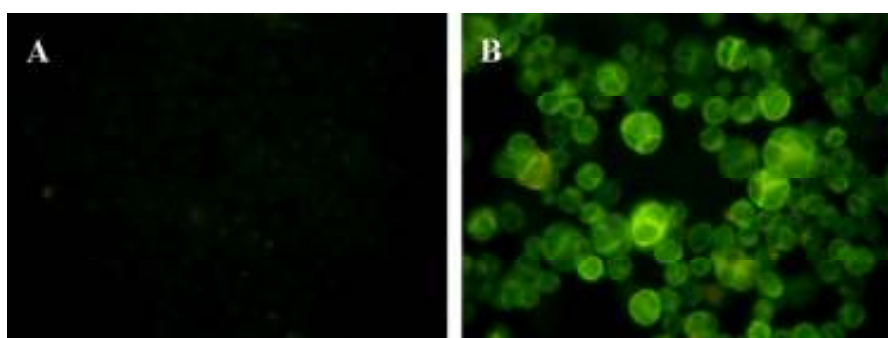


**Fig. 8.** Replication of HSV-1 in the SIRC cell line. SIRC cells were infected with the KOS strain of HSV-1 at an MOI of 1 for 48 h (B). Mock-infected SIRC cells cultured in parallel were left untreated (A). HSV-1 replication was examined by confocal microscopy.

MTT assays to evaluate the cytopathogenicity of HSV-1 revealed decreased viability at 48 hpi in 18, 44 and 44% of SIRC cells infected at MOIs of 0.1, 1 and 10, respectively (Fig. 9A). ELISA to evaluate the extent of apoptosis revealed increased apoptotic rates in

HSV-1-infected SIRC cells at 48 hpi; the EFs measured at MOIs of 0.1, 1 and 10 were 1.42, 4.35 and 5.8, respectively (Fig. 9B).

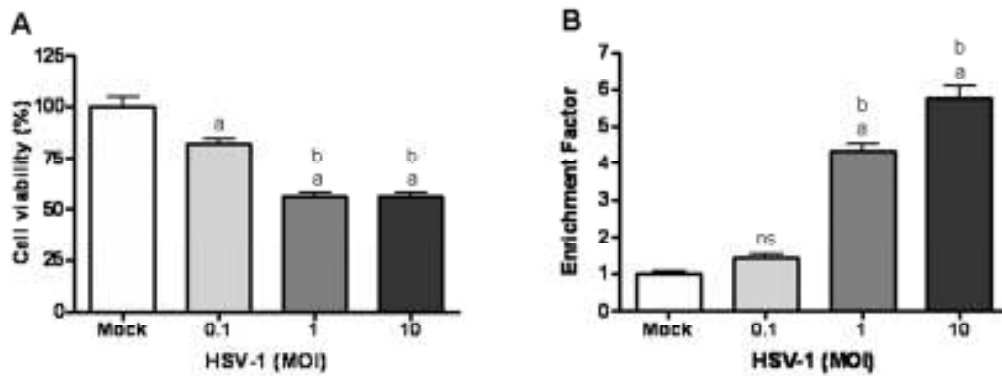


**Fig. 9.** HSV-1 induces cell death in the SIRC cell line. SIRC cells were infected with HSV-1 at different MOIs for 48 h. Mock-infected cells cultured in parallel were left untreated. The cell viability was measured by using the MTT assay (A). Apoptosis was detected by measuring the specific enrichment of mono- and oligonucleosomes in the cytoplasm by ELISA (B). <sup>a</sup> $P < 0.001$  vs. mock; <sup>b</sup> $P < 0.001$  vs. 0.1 MOI; ns = nonsignificant vs. mock.

Together, these data demonstrate the expression of HSV-1 gD protein that is consistent with efficient viral replication. Moreover, these results reveal that HSV-1 elicits a strong cytopathic effect in the SIRC cell line, and apoptosis plays an important role in the demise of the infected cells.

### I. B. 2. HSV-1 alters the levels of Bax and p63 proteins in SIRC cells

To determine whether HSV-1 can alter the expressions of Bax and p63, the steady-state levels of these proteins were determined by Western blot analysis. First, the kinetics of HSV-1 gD expression was investigated. The presence of gD was observed in the SIRC cell cultures infected with HSV-1 at an MOI of 10 at 12 hpi (Fig. 10; lane 20). The gD protein accumulated in the cultures infected with HSV-1 at MOIs of 0.1, 1 and 10 at 24 hpi (Fig. 10; lanes 23-25). High-level expression of the gD protein was also revealed in every culture infected with HSV-1 by 48 hpi (Fig. 10; lanes 27-30).

The analysis revealed the presence of a Bax isoform corresponding to Bax- $\beta$  in HSV-1-infected SIRC cultures at 12 hpi (the relative quantity of Bax- $\beta$  in cells infected at an MOI of 10 was 1.67) (Fig. 10; lane 20). At the 24-h time point, the expression of the Bax- $\beta$  protein in the HSV-1-infected SIRC cultures was upregulated (the relative quantities of Bax- $\beta$  in cells infected at MOIs of 1 and 10 were 6.42 and 8.31, respectively) (Fig. 10; lanes 24 and 25). At the 48-h time point, the HSV-1-infected SIRC cultures displayed elevated levels of Bax- $\beta$  (the

relative quantities of Bax- $\beta$  in cells infected at MOIs of 0.01, 0.1, 1 and 10 were 9.27, 9.93, 7.57 and 6.62, respectively) (Fig. 10; lanes 27-30).

The expression pattern of p63 was determined by using an antibody preparation which recognizes all of the various p63 isoforms. The analysis revealed the constitutive expression of a p63 protein migrating near 68 kDa in the mock-infected SIRC cells (lanes 1, 6, 11, 16, 21 and 26 in Fig. 10). Previously published data demonstrated that the 68 kDa protein possibly corresponds to  $\Delta$ Np63 $\alpha$  [92, 133]. At 12 hpi, the expression of  $\Delta$ Np63 $\alpha$  in the HSV-1-infected SIRC cultures was downregulated (the relative quantity of  $\Delta$ Np63 $\alpha$  in cells infected at an MOI of 10 was 0.87) (Fig. 10; lane 20). At the 24-h time point, HSV-1 triggered an impressive reduction in the level of  $\Delta$ Np63 $\alpha$  in the SIRC cells (the relative quantities in cells infected at MOIs of 0.1, 1 and 10 were 0.89, 0.43 and 0.41, respectively) (Fig. 10; lanes 23-25). At the 48-h time point, the HSV-1-infected SIRC cultures exhibited decreased levels of  $\Delta$ Np63 $\alpha$  (the relative quantities in cells infected at MOIs of 0.01, 0.1, 1 and 10 were 0.36, 0.22, 0.19 and 0.17, respectively) (Fig. 10; lanes 27-30).

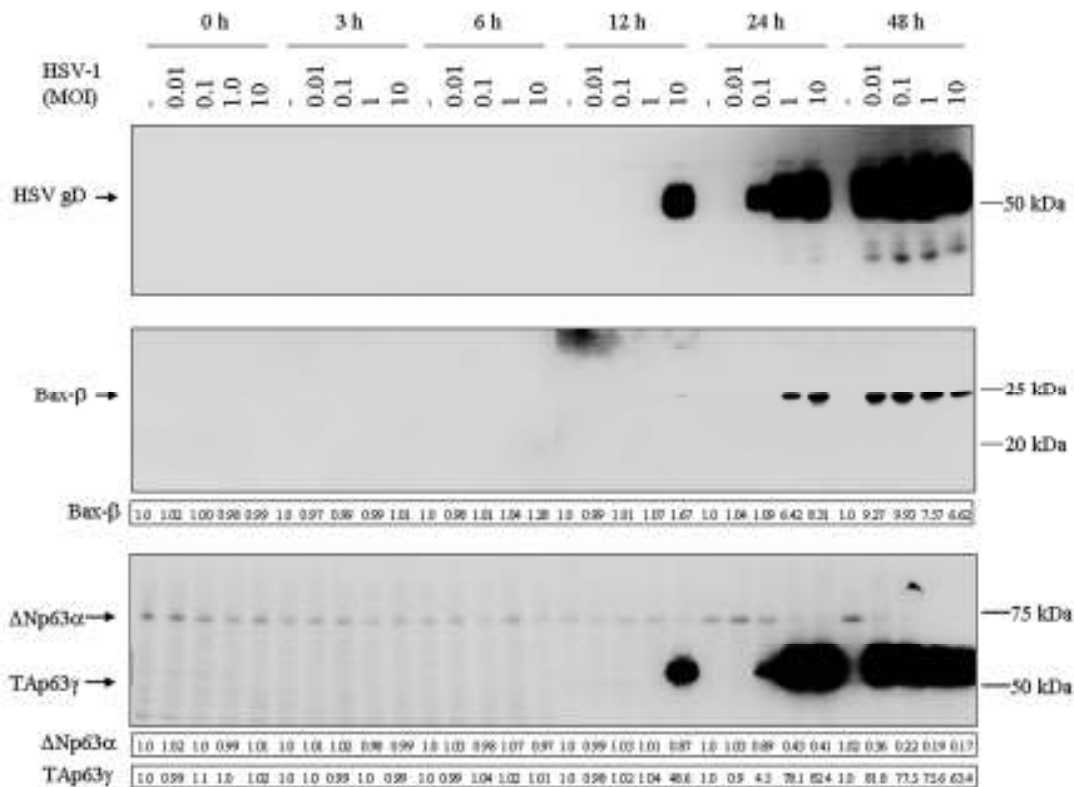


**Fig. 10.** HSV-1 infection alters the levels of p63 and Bax- $\beta$  in the SIRC cell line. The steady-state levels of proteins were analyzed by Western blot assay. To quantify protein levels in HSV-1-infected cells, band intensities were determined by densitometric analysis with the ImageQuant software. The numbers indicate the relative quantities of each band, normalized to the control cells at each time point.

The experiments also revealed the presence of a 51-62 kDa protein in HSV-1-infected SIRC cultures. Previously published data demonstrated that the 51-62 kDa protein possibly corresponds to TAp63 $\gamma$  [92, 133]. At 12 hpi, HSV-1-infected SIRC cells exhibited increased levels of TAp63 $\gamma$  (the relative quantity of TAp63 $\gamma$  in cells infected at an MOI of 10 was 48.6) (Fig. 10; lane 20). At the 24-h time point, the expression of TAp63 $\gamma$  in the HSV-1-infected SIRC cultures was highly upregulated (the relative quantities in cells infected at MOIs of 0.1, 1 and 10 were 4.5, 78.1 and 82.4) (Fig. 10; lanes 23-25). At 48-h postinfection, the HSV-1-infected SIRC cultures displayed elevated levels of TAp63 $\gamma$  (the relative quantities in cells infected at MOIs of 0.01, 0.1, 1 and 10 were 81.8, 77.5, 75.6 and 63.4, respectively) (Fig. 10; lanes 27-30).

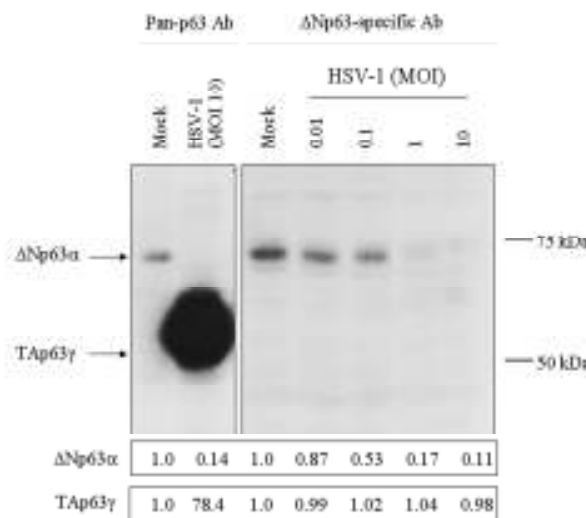


**Fig. 11.** Serological identification of the p63 isoforms expressed in HSV-1-infected SIRC cells. The levels of different p63 isoforms were detected at 24 hpi in mock-infected and HSV-1-infected SIRC cells by Western blot analysis, using an antibody preparation that recognizes all of the various p63 isoforms and a  $\Delta$ N-isoform-specific immunoglobulin.

To identify the p63 isoforms, the steady-state levels of these proteins were determined by Western blot analysis, using a polyclonal antiserum which reacts only with the  $\Delta$ N forms. The  $\Delta$ Np63-specific antibody preparation detected the 68 kDa p63 isoform in the mock-infected SIRC cells, but failed to recognize the 51-62 kDa p63 isoform in the cultures infected with HSV-1 at an MOI of 10 for 24 hpi (Fig. 11). These results clearly reveal that the 68 kDa p63 protein detected in the mock-infected SIRC cells is  $\Delta$ Np63 $\alpha$ , while the 51-62 kDa p63 isoform detected in HSV-1-infected cultures is TAp63 $\gamma$ .

Together, these results indicate that HSV-1 modulates the expression patterns of Bax and p63. The level of  $\Delta$ Np63 $\alpha$  was decreased, while the expressions of Bax- $\beta$  and TAp63 $\gamma$  were highly increased in the HSV-1-infected SIRC cells.

### I. B. 3. HSV-1-mediated TAp63 $\gamma$ expression requires viral DNA replication in SIRC cell line

To investigate the basis of the HSV-1-induced increase of the TAp63 $\gamma$  level, SIRC cells were infected in the presence or absence of the viral DNA replication inhibitor ACG. The cells were analyzed for the presence of HSV gD,  $\Delta$ Np63 $\alpha$ , TAp63 $\gamma$  and Bax- $\beta$ . The low level of the late protein gD expression in SIRC samples treated with 50 or 10  $\mu$ g/ml ACG indicated that the drug treatment efficiently inhibited viral DNA replication (Fig. 12; lanes 2 and 3).

The Bax- $\beta$  protein levels in the HSV-1-infected SIRC cells treated with 50, 10 and 1  $\mu$ g/ml ACG were greatly decreased (the relative quantities of Bax- $\beta$  in cells infected at an MOI of 10 were 0.12, 0.15 and 0.21, respectively) (Fig. 12; lanes 2-4).

The TAp63 $\gamma$  protein levels in the HSV-1-infected SIRC cells treated with 50 and 10  $\mu$ g/ml ACG were greatly decreased (the relative quantities of TAp63 $\gamma$  in cells infected at an MOI of 10 were 0.11 and 0.19) (Fig. 12; lanes 2 and 3). The expression of the TAp63 $\gamma$  isoform in the HSV-1-infected cultures treated with 1  $\mu$ g/ml ACG was downregulated (the relative quantity of TAp63 $\gamma$  in SIRC cells infected at an MOI of 10 was 0.24) (Fig. 12; lane 4).

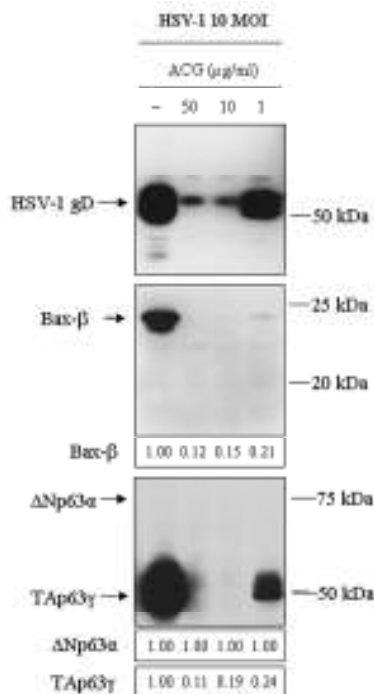


**Fig. 12.** The HSV-1-mediated TAp63 $\gamma$  expression requires viral DNA replication. SIRC cells were infected with the KOS strain of HSV-1 at an MOI of 10 and maintained for 24h in the absence or in the presence of ACG. The steady-state levels of Bax and p63 isoforms were analyzed by Western blot assay. To quantify protein levels in HSV-1-infected cells, band intensities were determined by densitometric analysis with the ImageQuant software. The

numbers indicate the relative quantities of each band, normalized to the control cells at each time point.

## *II. The effects of VSV infection on the expression patterns of p63 and Bax in HaCaT cells*

### **II. 1. The HaCaT cell line is permissive for VSV replication**

To determine whether VSV multiplies in the HaCaT cell line, different methods were used. Indirect immunofluorescence assays revealed positive staining for VSV G protein at 48 h after virus inoculation in  $\geq 98\%$  of the cells infected at an MOI of 1 (Fig. 13A). Western blot analyses revealed the presence of the G protein in cultures infected at MOIs of 0.1 and 1 at 24 h after VSV inoculation (Fig. 13B). By 48 h, the G protein had accumulated in every culture infected with VSV (Fig. 13B).

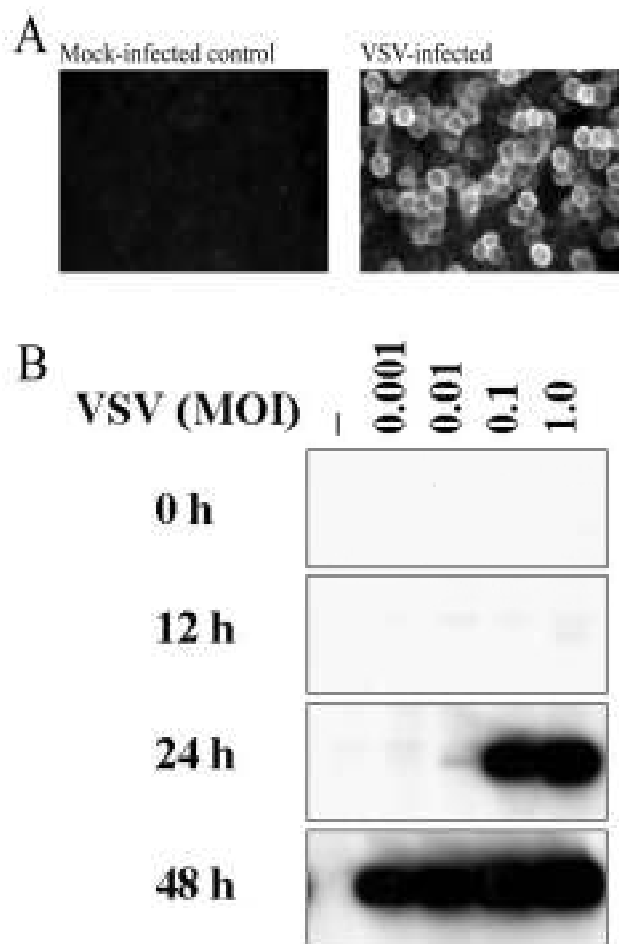


**Fig. 13.** VSV replication in the HaCaT keratinocyte cell line. (A) HaCaT cells were infected with the Indiana strain of VSV at an MOI of 1 for 48 h. Mock-infected cells cultured in parallel were left untreated. VSV replication was examined by confocal microscopy. (B) The steady-state level of VSV G protein was analyzed by Western blot assay.

The progeny virus production was determined by plaque titration of the culture supernatants taken from HaCaT cells at 12, 24, 48 and 72 hpi. Depending on the infectious



dose, the level of VSV production varied between  $3.0 \times 10^3$  and  $1.9 \times 10^6$  PFU/ml at 12 hpi (Table 2). The virus titers thereafter increased, and ranged from  $4.5 \times 10^5$  to  $4.6 \times 10^7$  PFU/ml at 24 h after virus inoculation (Table 2). The level of virus production varied between  $2.6 \times 10^7$  and  $6.4 \times 10^7$  PFU/ml at 48 hpi (Table 2). The VSV production of cells infected with various MOIs rose to titers of about  $2 \times 10^8$  PFU/ml after 72 h of culturing (Table 2).

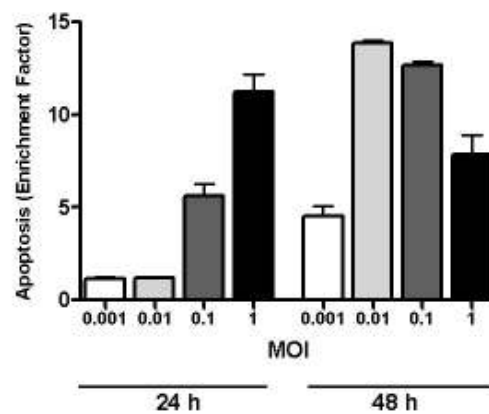
Accordingly, the maximum yield at 0.001, 0.01, 0.1 and 1 MOI corresponded to 1300, 1400, 1200, and 1000 PFU/cell, respectively. Together, these data clearly demonstrate that VSV replicates efficiently in the HaCaT keratinocyte cell line.

Table 2. Viral titers in VSV-infected HaCaT cells

MOI	Titer of VSV (PFU/ml)			
	12 h	24 h	48 h	72 h
0.001	$3.0 \times 10^3$	$4.5 \times 10^5$	$2.6 \times 10^7$	$2.6 \times 10^8$
0.01	$1.5 \times 10^4$	$3.6 \times 10^6$	$2.8 \times 10^7$	$2.8 \times 10^8$
0.1	$1.5 \times 10^5$	$1.7 \times 10^7$	$3.8 \times 10^7$	$2.4 \times 10^8$
1.0	$1.9 \times 10^6$	$4.6 \times 10^7$	$6.4 \times 10^7$	$2.0 \times 10^8$

## II. 2. VSV induces apoptosis in the HaCaT cell line

To investigate the ability of VSV to induce apoptosis in HaCaT cells, the extent of histones complexed with mono- and oligonucleosome fragments was measured by ELISA. At 24 h after virus inoculation, the EFs measured in cells infected at MOIs of 0.001, 0.01, 0.1 and 1 MOI were 1.2, 1.2, 5.6 and 11.2, respectively (Fig. 14). At 48 h after infection, the EFs measured in cells infected at MOIs of 0.001, 0.01, 0.1 and 1 MOI were 4.5, 13.8, 12.7 and 7.9, respectively (Fig. 14). These data indicate that VSV elicits apoptosis in HaCaT cells.



**Fig. 14.** VSV induces apoptosis in the HaCaT keratinocyte cell line. VSV-induced apoptosis was measured by ELISA in HaCaT cells in comparison with the corresponding mock-infected control.

### II. 3. VSV infection alters the levels of $\Delta$ Np63 $\alpha$ , p53<sup>mt</sup>, p21 Bax and p18 Bax proteins in the HaCaT cell line

To determine whether VSV infection can alter the expressions of proteins involved in apoptosis, the steady-state levels of  $\Delta$ Np63 $\alpha$ , p53<sup>mt</sup>, p21 Bax and p18 Bax were measured by Western blot assay. The analysis revealed the endogenous expression of  $\Delta$ Np63 $\alpha$ , p53<sup>mt</sup> and p21 Bax in mock-infected HaCaT cells (Fig. 15; lanes 1, 6 and 11). The endogenous expression of  $\Delta$ Np63 $\alpha$  in mock-infected cells remained constant throughout the 48 h of culturing (Fig. 15; lanes 1, 6 and 11).

The VSV-infected cells exhibited decreased levels of  $\Delta$ Np63 $\alpha$  at 24 h after virus inoculation. The relative quantities of  $\Delta$ Np63 $\alpha$  were 0.84 and 0.7 in cells infected at MOIs of 0.1 and 1, respectively. (Fig. 15; lanes 9 and 10). The expression of  $\Delta$ Np63 $\alpha$  protein in the VSV-infected cultures at the 48 h time point was downregulated. The relative quantities of  $\Delta$ Np63 $\alpha$  were 0.44, 0.12, 0.08 and 0.08 in cells infected at MOIs of 0.001, 0.01, 0.1 and 1, respectively (Fig. 15; lanes 12-15).

The endogenous expression of p53<sup>mt</sup> in mock-infected cells similarly remained constant throughout 48 h of culturing (Fig. 15; lanes 1, 6, and 11). No quantitative differences between the VSV-infected and control cultures were observed in the level of expression of p53<sup>mt</sup> protein at the 24 h time point (Fig. 15; lanes 7-10 and 6, respectively). The expression of p53<sup>mt</sup> in VSV-infected cultures at 48 h after VSV inoculation was downregulated (the relative quantities of p53<sup>mt</sup> were 0.83 and 0.4 in cells infected at MOIs of 0.1 and 1, respectively) (Fig. 15; lanes 14 and 15).

The endogenous expression of p21 Bax in mock-infected cells likewise remained constant in the course of the 48 h of culturing (Fig. 15; lanes 1, 6, and 11). No quantitative differences between the VSV-infected and control cultures were displayed in the level of expression of p21 Bax protein at the 24 h time point (Fig. 15; lanes 7-10 and 6, respectively). The expression of p21 Bax in VSV-infected cells at 48 h after inoculation was upregulated (the relative quantities of p21 Bax were 1.33 and 1.53 in cells infected at MOIs of 0.1 and 1, respectively) (Fig. 15; lanes 14 and 15).

Furthermore, VSV-infected cells exhibited increased levels of p18 Bax at 48 h after inoculation (the relative quantities of p18 Bax were 2.32, 8.64, 14.8 and 17.7 in cells infected at MOIs of 0.001, 0.01, 0.1 and 1, respectively) (Fig. 15; lanes 12-15). Together, these data indicate that the expressions of  $\Delta$ Np63 $\alpha$ , p53<sup>mt</sup>, p21 Bax and p18 Bax are differentially modulated by VSV.

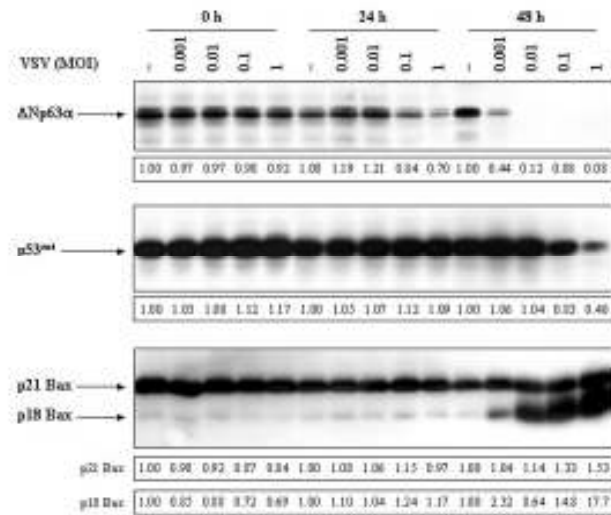


**Fig. 15.** VSV infection differentially modulates the levels of  $\Delta Np63\alpha$ ,  $p53^{mt}$ , p21 Bax and p18 Bax in the HaCaT keratinocyte cell line. The steady-state levels of proteins were analyzed by Western blot assay. To quantify protein levels in VSV-infected cells, band intensities were determined by densitometric analysis with the ImageQuant software. The numbers indicate the relative quantities of each band, normalized to the control cells at each time point.

## DISCUSSION

### The effects of HSV infection on the expression patterns of p63, p73 and Bax in primary keratinocytes, HaCaT and SIRC cells

In an effort to gain more insight into the pathogenic mechanisms of skin and ocular surface infections caused by HSV-1 and HSV-2, we set out to investigate the effects of these viruses on the levels of p63, p73 and Bax expression.

Our data revealed that HSV-1 replicated to high titers and triggered a strong cytopathic effect in the HaCaT and SIRC cell lines (Table 1 and Fig. 3A). Furthermore, apoptosis played an important role in the demise of the infected keratinocytes and cornea epithelial cells (Fig. 3B).

Consistently with previous findings [134, 135], we found that several p63 isoforms can be detected both in the HaCaT cell line and in primary keratinocytes, and that  $\Delta Np63\alpha$  is the predominant isoform, migrating as a doublet due to its post-translational modification by phosphorylation (Figs 4 and 5). For the first time, our experiments have also revealed the constitutive expression of  $\Delta Np63\alpha$  in the rabbit corneal SIRC cell line (Figs 10 and 11).

Interestingly, HSV-1 triggered an impressive reduction in the level of the  $\Delta Np63\alpha$  doublet and a dramatic increase in the expression of TAp63 $\gamma$  (Figs 4, 5 and 10). The kinetics of HSV-1 replication and the alteration in the stoichiometric ratio of the p63 isoforms correlated strictly (Table 1, Figs 4, 5 and 10). We additionally investigated the biological impact of the HSV-1-mediated accumulation of TAp63 $\gamma$  by using siRNA technology (Fig. 7).

Our experiments revealed that the knockdown of TAp63 expression increases the viability of infected HaCaT cells (Fig. 7B), suggesting that TAp63 $\gamma$  may play some role in the complex mechanisms involved in the cytopathogenicity of HSV-1. Noteworthy previous studies raise the possibility that HSV-1 may alter the expression of p63 via multiple mechanisms [136-144]. Certain viral proteins may have the potential to alter the transcription of p63 or to affect the stability and activity of the p63 isoforms via the induction of their posttranslational modifications [136-144]. The virion-associated host shutoff protein [(vhs), also known as UL41], which causes the degradation of cellular and viral RNA [136, 137], may evoke a decrease in the level of  $\Delta$ Np63 $\alpha$  mRNA. The  $\alpha$ -trans-inducing factor [( $\alpha$ -TIF), also known as VP16 or UL48], which stimulates the transcription of IE genes via cellular transcription factors, such as the POU homeodomain protein Oct-1 (where Oct stands for octamer binding protein) and the host cell factor [138-140], may elicit an increase in the level of TAp63 $\gamma$ . The infected cell protein (ICP) 0, which controls the stability of cellular proteins and leads to the disruption of promyelocytic leukemia (PML) nuclear bodies [also known as PODs (PML oncogenic domains) and ND10 (nuclear domain 10)] [141-144], may dysregulate the expression pattern of p63. Other interesting recent studies have also revealed that HSV genome synthesis activates the cellular DNA damage response [145-149]. While HSV disrupts the ataxia teleangiectasia mutated- and rad3-related (ATR) pathway, it activates and even exploits the ataxia teleangiectasia mutated (ATM)-dependent signaling cascade to support its own replication [147, 149]. Both ATM and ATR belong in the family of phosphatidylinositol 3-kinase-like kinases (PIKKs) and function as part of a complex response to DNA damage [149]. Via phosphorylation, PIKKs activate multiple proteins, including the p53 family members [149]. Recent observations indicate that genotoxic stress induces the accelerated degradation of  $\Delta$ Np63 and the accumulation of TAp63 isoforms; in turn, these function as downstream mediators of the cellular DNA damage response, to provide time for repair or to kill cells bearing irreparable DNA damage and unstable genome by inducing apoptotic demise [112, 150-152]. Our experiments have demonstrated that the viral DNA replication inhibitor ACG completely abolished the HSV-1-mediated induction of TAp63 $\gamma$  in both HaCaT and SIRC cells, indicating that replication of viral DNA is necessary for the accumulation of TAp63 $\gamma$  (Figs 6 and 12). This observation strongly supports the view that the dysregulation of p63 expression depends on the cellular DDR, but does not exclude the role of HSV-1-encoded proteins. Thus, additional studies are required to elucidate the potential contributions of vhs,  $\alpha$ -TIF, ICP0 and other viral proteins to the development of the HSV-1-mediated dysregulation of p63 expression.

In line with these data, we next investigated the expression of the p53 family member p73. Similar to *p63*, the *p73* gene has two transcription start sites, producing two p73 subclasses: the TA and  $\Delta N$  isoforms. In addition to these amino-terminal differences, alternative splicing generates seven carboxy-terminal variants, denoted  $\alpha$ ,  $\beta$ ,  $\gamma$ ,  $\delta$ ,  $\epsilon$ ,  $\zeta$  and  $\eta$ . The TAp73 isoforms transactivate a variety of p53 and p73 target genes and induce apoptosis, while the  $\Delta Np73$  isoforms possess little transcriptional activity, display dominant negative behavior and inhibit apoptosis [153]. Our studies have shown that the level of a 50 kDa p73 isoform was decreased, while the expression of a 44.5 kDa p73 protein was increased in HaCaT cells following HSV-1 infection (Fig. 4). On the basis of previously published data we suggest that the p73 isoforms migrating near 50 and 44.5 kDa may correspond to  $\Delta Np73\beta$  and TAp73 $\delta$ , respectively [106, 153]. However, further studies are required for the clear-cut identification of the p73 isoforms detected in HaCaT keratinocytes. Together, these data demonstrate that HSV-1 dysregulates the expression pattern of p73 in the HaCaT cell line.

In order to gain more insight into the stress response triggered by HSV-1, we also studied the expression of Bax, which is known to be upregulated by TAp63 $\alpha$  and TAp63 $\gamma$  [99, 105]. Previous studies have demonstrated the existence of several Bax isoforms [125]. It is well documented that Bax- $\alpha$  is a central component of apoptosis induction [111]. In response to apoptotic stimuli, Bax- $\alpha$  becomes activated, translocates to the mitochondria and triggers the release of cytochrome *c* and caspase-9, which in turn results in the irreversible execution of the apoptotic program [154]. It has also been reported that the Bax- $\beta$  protein is expressed constitutively in several human cell types, and its level is controlled by proteasomal degradation [126]. Various stressors inhibit ubiquitination of the Bax- $\beta$  protein and thereby prevent its proteasomal degradation, leading to the accumulation of this Bax isoform [126]. Similarly to Bax- $\alpha$ , Bax- $\beta$  has the capability to trigger apoptosis via the mitochondrial pathway [126, 127]. Moreover, Bax- $\beta$  associates with and promotes Bax- $\alpha$  activation [127]. Our experiments revealed no alterations in the expression of Bax- $\alpha$  (Figs 4, 5 and 10). Interestingly, we observed a dramatic rise in the level of Bax- $\beta$  in HSV-1-infected HaCaT and SIRC cultures (Figs 4 and 10). Following the demonstration of an altered Bax expression pattern in the HaCaT and SIRC cells, we postulate an important role for Bax- $\beta$  in the apoptotic responsiveness of keratinocytes and corneal epithelial cells infected with HSV-1. Other interesting recent data have proved that HSVs encode ubiquitinating and deubiquitinating enzymes, which can modify the ubiquitination status of both viral and host cell proteins [155, 156]. In view of these observations, it is reasonable to infer that the Bax- $\beta$  protein may be a novel target of HSV-1-mediated deubiquitinating events. However, the

precise molecular mechanisms responsible for stabilization of the Bax- $\beta$  protein in HSV-1-infected cells remain to be elucidated.

A great body of experimental evidence indicates that the cellular responses triggered by HSV-1 or HSV-2 display both various similarities and profound differences [1, 3, 5]. It has been clearly proved that HSV-1 and HSV-2 differ in their nucleotide sequences and rates of reactivation, and also in the cellular transcriptional responses and spectrum of diseases they evoke. Interesting previous studies have also revealed fundamental differences between HSV-1 and HSV-2 in their apoptosis-modulating effect [157]. Accordingly, we examined the expression patterns of the p63, p73 and Bax isoforms and determined the proportion of apoptotic HaCaT keratinocytes after infection with HSV-2. Although the proportions of dead cells were comparable in the HSV-1- and HSV-2-infected cultures, the early apoptotic population was larger in the cultures infected with HSV-1 than in those infected with HSV-2 (Fig. 3). These data raise the possibility that HSV-1-infected keratinocytes, displaying highly elevated TAp63 $\gamma$  levels, may be prone to commit apoptosis, while HSV-2-infected cells may rather be disposed to die by way of necrosis or autophagy. Similarly as in the case of HSV-1, HSV-2-infected HaCaT cultures exhibited impressive reductions in the expressions of  $\Delta$ Np63 $\alpha$  and the 50 kDa p73 isoform; unexpectedly, however, the level of TAp63 $\gamma$  remained unaffected and the expression of a 44.5 kDa p73 isoform was decreased in HSV-2-infected HaCaT keratinocytes (Fig. 4). HSV-2 infection further resulted in a very slight increase in the expression of Bax- $\beta$ , the magnitude of which proved to be much lower than that observed after HSV-1 infection (Fig. 4).

Taken together, our results indicate that both HSV-1 and HSV-2 replicate efficiently and elicit powerful cytopathogenicity, and apoptosis plays an important role in the demise of the infected keratinocytes and corneal epithelial cells. For the first time, our data also demonstrate that HSV-1 and HSV-2 modulate the patterns of p63, p73 and Bax expression in a serotype-specific manner. The dysregulated pattern of p63 expression observed in HSV-infected HaCaT and SIRC cultures may comprise part of a mechanism by which these viruses perturb the functions of epithelial cells and lead to their demise. These data may bear on the pathogenic mechanisms of diseases caused by HSV-1 and HSV-2, as p63 isoforms play a pivotal role in the epithelial homeostasis.

### **The effects of VSV infection on the expression patterns of p63 and Bax in HaCaT cells**

In an effort to evaluate the potential oncolytic activity of VSV in epithelial-derived skin cancers, we set out to investigate the cytopathogenicity of this virus in the immortalized HaCaT keratinocyte cell line.

Our data revealed that VSV was able to establish an infection, affecting virtually all of the cells and yielding high titers of progeny virus (Fig. 13 and Table 2). VSV infection elicited a strong cytopathic effect (data not shown) and apoptosis (Fig. 14), leading to the demise of cultures within 72 h. For the first time, our data clearly demonstrated the susceptibility of immortalized keratinocytes to the deadly infection caused by VSV.

Interestingly, we observed an impressive reduction of the  $\Delta$ Np63 $\alpha$  level of VSV-infected cells (Fig. 15). It is important that the kinetics of VSV replication, apoptosis and suppression of  $\Delta$ Np63 $\alpha$  expression correlated strictly (Figs 13-15 and Table 2). This suggests that the VSV-induced decrease in  $\Delta$ Np63 $\alpha$  levels is a key event in the apoptotic response of the infected keratinocytes.

Consistent with previous results [158], our experiments have shown that the HaCaT cell line accumulates high amounts of p53<sup>mt</sup> (Fig. 15). Our further experiments revealed that VSV infection decreases the level of p53<sup>mt</sup> (Fig. 15). Since apoptosis was detected in infected cultures displaying unaffected levels of p53<sup>mt</sup> (Figs 14 and 15), the downregulation of p53<sup>mt</sup> expression does not seem to be involved in the induction of apoptosis; it may rather operate in the executional phase and contribute to the inevitable death of heavily infected cells.

In line with these data, we investigated the expression of Bax isoforms. Our experiments revealed the endogenous expression of a ~21 kDa Bax isoform in the HaCaT cell line (Fig. 15). Previously published data suggest that p21 Bax is identical with Bax- $\alpha$  [159]. Interestingly, we observed high increases in the levels of Bax- $\alpha$  and p18 Bax in VSV-infected HaCaT cultures (Fig. 15). Recent data have shown that the activity of Bax- $\alpha$  is subject to regulation by calpain-mediated proteolytic cleavage in cells exposed to stress, such as irradiation, etoposide or cisplatin treatment [131, 160]. Cleavage of Bax- $\alpha$  was shown to yield a p18 Bax product, which behaves like a sensitizer type of BH3-only proteins [141]. The p18 truncated form of Bax- $\alpha$  is more potent in disrupting mitochondrial integrity and inducing apoptosis [130, 131, 160]. Thus, the dramatic rises detected in the levels of Bax- $\alpha$  and p18 Bax in HaCaT cells following VSV infection are indicative of a pro-apoptotic shift and may be of importance in the amplification of the apoptotic process, and contribute to the powerful cytopathogenicity of this virus.

Taken together, our results demonstrate for the first time that VSV replicates efficiently and triggers apoptosis in the immortalized HaCaT keratinocyte cell line. The VSV-mediated alterations in the expressions of  $\Delta$ Np63 $\alpha$  and Bax may be implicated in the apoptotic demise of infected cells and may also sensitize to other apoptotic stimuli. Our findings extend the known spectrum of cell types susceptible for the powerful oncolytic

activity of VSV to immortalized keratinocytes. These observations may stimulate further studies aimed at the development of VSV-based virotherapy into an effective modality for the treatment of epithelial-derived tumors of the skin.

## SUMMARY

In light of the critical role of p63 in the epithelial cell fate, we considered the question of whether HSV-1, HSV-2 and VSV affect the patterns of p63 and Bax expression.

Our results have revealed that both HSV-1 and HSV-2 replicated efficiently, and elicited a strong cytopathic effect, and apoptosis played an important role in the demise of the infected primary keratinocytes, HaCaT and SIRC cells. The level of  $\Delta\text{Np63}\alpha$  was decreased, Bax- $\alpha$  remained unaffected, while the expressions of the Bax- $\beta$  and TAp63 $\gamma$  isoforms were highly increased in HSV-1-infected primary keratinocytes, HaCaT and SIRC cells. In contrast, in response to HSV-2 infection the level of  $\Delta\text{Np63}\alpha$  was decreased, Bax- $\alpha$  and TAp63 $\gamma$  remained unaffected, while the expression of Bax- $\beta$  was slightly increased in HaCaT keratinocytes. The knockdown of TAp63 expression enhanced the viability of HSV-1-infected cells. Thus, HSV-1 and HSV-2 modulate the patterns of p63 and Bax expression in a serotype-specific manner. The dysregulated pattern of p63 expression observed in HSV-infected HaCaT and SIRC cultures may comprise part of a mechanism by which these viruses perturb the functions of epithelial cells and lead to their demise. By disturbing the delicate balance between the pro-survival  $\Delta\text{N}$  and the pro-apoptotic TA isoforms, HSV-1 and HSV-2 may cause profound alterations in the tissue homeostasis of the skin and the ocular surface.

Our results have demonstrated that VSV replicated efficiently, and elicited a strong cytopathic effect leading to the demise of immortalized HaCaT keratinocytes. The cytopathogenicity evoked by VSV was linked to apoptotic mechanisms. The levels of  $\Delta\text{Np63}\alpha$  and p53<sup>mt</sup> were decreased, while the expressions of Bax- $\alpha$  and p18 Bax were increased in VSV-infected HaCaT cells. The VSV-mediated alterations in the expressions of  $\Delta\text{Np63}\alpha$  and Bax may be implicated in the apoptotic demise of infected cells and may also sensitize to other apoptotic stimuli. Our findings extend the known spectrum of cell types susceptible for the powerful oncolytic activity of VSV to immortalized keratinocytes. These observations may stimulate further studies aimed at the development of VSV-based virotherapy into an effective modality for the treatment of epithelial-derived tumors of the skin.



## ACKNOWLEDGEMENTS

This work has been carried out at the Department of Medical Microbiology and Immunobiology, Faculty of Medicine, University of Szeged.

I am deeply indebted to my supervisor, **Associate Professor Klára Megyeri**, who has helped me with good sense, unfailing efficiency and friendly encouragement. She has made the enterprise of research work a challenge, as well as an education for me. I am also very grateful to her for useful advice and for critical reading of the manuscript.

I greatly acknowledge **Professor Yvette Mándi**, Head of the Department of Medical Microbiology and Immunobiology for providing working facilities and for her support and advice.

My warmest thanks are due to **Professor Lajos Kemény** for the significant help.

I would like to acknowledge the support of **Professor Norbert E. Fusenig**.

I also thank **Gyöngyi Ábrahám** for her excellent technical assistance and advice.

I owe much to my colleagues, especially **Dr. Éva Gallyas, Dr. Andrea Facskó, Prof. Zsuzsanna Bata-Csörgő, Dr. György Seprényi, Katalin Pásztor, Dr. Béla Taródi, Dr. Imre Ocsovszki and Bernadett Kormos** for pleasant cooperation.

I thank **all my colleagues** at the Department of Medical Microbiology and Immunobiology for their support and for creating a pleasant work-environment.

I record my gratitude to **my family** for their love, support and understanding.

The financial support received from grants OTKA/T043144 by the Hungarian Scientific Research Fund and ETT/398/2003 by the Hungarian Ministry of Health, Social and Family Affairs is gratefully acknowledged.

## REFERENCES

1. Roizman, B., Sears, A. E. (1996). Herpes simplex viruses and their replication. In: Fields, B. N., Knipe, D. M., Howley, P. M., Chanock, R. M., Melnick, J. L., Monath, T. P., Roizman, B., Straus S. E. (Eds.), "*Fields Virology*", 3<sup>rd</sup> ed., pp. 2231-2295. Lippincott-Raven, Philadelphia.
2. Taylor, T. J., Brockman, M. A., McNamee, E. E., Knipe, D. M. (2002). Herpes simplex virus. *Front. Biosci.* **7**, 752-764.
3. Taddeo, B., Esclatine, A., Roizman, B. (2002). The patterns of accumulation of cellular RNAs in cells infected with a wild-type and a mutant herpes simplex virus 1 lacking the virion host shutoff gene. *P. Natl. Acad. Sci. USA* **99**, 17031-17036.
4. Roizman, B., Gu, H., Mandel, G. (2005). The first 30 minutes in the life of a virus: unrest in the nucleus. *Cell Cycle* **4**, 1019-1021.
5. Kamakura, M., Nawa, A., Ushijima, Y. Goshima, F., Kawaguchi, Y., Kikkawa, F., Nishiyama, Y. (2008). Microarray analysis of transcriptional responses to infection by herpes simplex virus types 1 and 2 and their US3-deficient mutants. *Microbes Infect.* **10**, 405-413.
6. Biederer, C., Ries, S., Brandts, C. H., McCormick, F. (2002). Replication-selective viruses for cancer therapy. *J. Mol. Med.* **80**, 163-175.
7. Ring, C. J. A. (2002). Cytolytic viruses as potential anti-cancer agents. *J. Gen. Virol.* **83**, 491-502.
8. Balachandran, S., Porosnicu, M., Barber, G. N. (2001). Oncolytic activity of *vesicular stomatitis virus* is effective against tumors exhibiting aberrant p53, Ras, or Myc function and involves the induction of apoptosis. *J. Virol.* **75**, 3474-3479.
9. Fernandez, M., Porosnicu, M., Markovic, D., Barber, G. N. (2002). Genetically engineered *vesicular stomatitis virus* in gene therapy: application for treatment of malignant disease. *J. Virol.* **76**, 895-904.
10. Biswas, P. S., Rouse, B. T. (2005). Early events in HSV keratitis—setting the stage for a blinding disease. *Microbes Infect.* **7**, 799-810.
11. Koyama, A. H., Adachi, A. (1997). Induction of apoptosis by herpes simplex virus type 1. *J. Gen. Virol.* **78**, 2909-2912.
12. Koyama, A. H., Akari, H., Adachi, A., Goshima, F., Nishiyama, Y. (1998). Induction of apoptosis in Hep-2 cells by infection with herpes simplex virus type 2. *Arch. Virol.* **143**, 2435-2441.

13. Galvan, V., Roizman, B. (1998). Herpes simplex virus 1 induces and blocks apoptosis at multiple steps during infection and protects cells from exogenous inducers in a cell-type-dependent manner. *P. Natl. Acad. Sci. USA* **95**, 3931-3936.
14. Aubert, M., O'Toole, J., Blaho, J. A. (1999). Induction and prevention of apoptosis in human Hep-2 cells by herpes simplex virus type 1. *J. Virol.* **73**, 10359-10370.
15. Aubert, M., Blaho, J. A. (2001). Modulation of apoptosis during herpes simplex virus infection in human cells, *Microbes Infect.* **3**, 859-866.
16. McLean, J. E., Ruck, A., Shirazian, A., Pooyaei-Mehr, F., Zakeri, Z. F. (2008). Viral manipulation of cell death. *Curr. Pharm. Des.* **14**, 198-220.
17. Megyeri, K. (2007). Modulation of apoptotic pathways by herpes simplex viruses. In: Minarovits, J., Gonczol, E., Valyi-Nagy T. (Eds.), "*Latency Strategies of Herpesviruses*", 1<sup>st</sup> ed., pp. 37-54. Springer, New York.
18. Orvedahl, A., Levine, B. (2008). Autophagy and viral neurovirulence. *Cell. Microbiol.* **10**, 1747-1756.
19. Duprez, L., Wirawan, E., Vanden Berghe, T., Vandenabeele, P. (2009). Major cell death pathways at a glance. *Microbes Infect.* **11**, 1050-1062.
20. Roulston, A., Marcellus, R. C., Branton, P. E. (1999). Viruses and apoptosis. *Annu. Rev. Microbiol.* **53**, 577-628.
21. Hay, S., Kannourakis, G. (2002). A time to kill: viral manipulation of the cell death program. *J. Gen. Virol.* **83**, 1547-1564.
22. Chiarugi, P., Giannoni, E. (2008). Anoikis: a necessary death program for anchorage-dependent cells. *Biochem. Pharmacol.* **76**, 1352-1364.
23. Labbé, K., Saleh, M. (2008). Cell death in the host response to infection. *Cell Death Differ.* **15**, 1339-1349.
24. Galluzzi, L., Kroemer, G. (2008). Necroptosis: a specialized pathway of programmed necrosis. *Cell* **135**, 1161-1163.
25. Espert, L., Codogno, P., Biard-Piechaczyk, M. (2007). Involvement of autophagy in viral infections: antiviral function and subversion by viruses. *J. Mol. Med.* **85**, 811-823.
26. Whitley, R. J., Roizman, B. (2001). Herpes simplex virus infections. *Lancet* **357**, 1513-1518.
27. Spear, P. G. (2004). Herpes simplex virus: receptors and ligands for cell entry. *Cell. Microbiol.* **6**, 401-410.
28. Garner, J. A. (2003). Herpes simplex virion entry into and intracellular transport within mammalian cells. *Adv. Drug Deliver. Rev.* **55**, 1497-1513.

29. Whitley, R. J. (1996). Herpes simplex viruses. In: Fields, B. N., Knipe, D. M., Howley, P. M., Chanock, R. M., Melnick, J. L., Monath, T. P., Roizman, B., Straus S. E. (Eds.), "*Fields Virology*", 3<sup>rd</sup> ed., pp. 2297-2342. Lippincott-Raven, Philadelphia.
30. Roizman, B., Pellett, P. E. (2001). The family Herpesviridae: a brief introduction. In: Knipe, D. M., Howley, P. M. (Eds.), "*Fields Virology*", 4<sup>th</sup> ed., pp. 2381-2397. Lippincott Williams & Wilkins, Philadelphia.
31. Nguyen, M. L., Blaho, J. A. (2007). Apoptosis during herpes simplex virus infection. *Adv. Virus Res.* **69**, 67-97.
32. Galvan, V., Brandimarti, R., Roizman, B. (1999). Herpes simplex virus 1 blocks caspase-3-independent and caspase-dependent pathways to cell death. *J. Virol.* **73**, 3219-3226.
33. Wu, N., Watkins, S. C., Schaffer P. A., DeLuca, N. A. (1996). Prolonged gene expression and cell survival after infection by a herpes simplex virus mutant defective in the immediate-early genes encoding ICP4, ICP27, and ICP22. *J. Virol.* **70**, 6358-6369.
34. Lia, H., Baskaran, R., Krisky, D. M., Bein, K., Grandi, P., Cohen, J. B., Joseph C. Glorioso, J. C. (2008). Chk2 is required for HSV-1 ICP0-mediated G2/M arrest and enhancement of virus growth. *Virology* **375**, 13-23.
35. Hobbs, W. E., DeLuca, N. A. (1999). Perturbation of cell cycle progression and cellular gene expression as a function of herpes simplex virus ICP0. *J. Virol.* **73**, 8245-8255.
36. Aubert, M., Pomeranz, L. E., Blaho, J. A. (2007). Herpes simplex virus blocks apoptosis by precluding mitochondrial cytochrome c release independent of caspase activation in infected human epithelial cells. *Apoptosis* **12**, 19-35.
37. Tallóczy, Z., Virgin, W. H., Levine, B. (2006). PKR-dependent autophagic degradation of Herpes simplex virus type 1. *Autophagy* **2**:24-29.
38. Deshmane, S. L., Fraser, N. W. (1989). During latency, herpes simplex virus type 1 DNA is associated with nucleosomes in a chromatin structure. *J. Virol.* **63**, 943-947.
39. Kaye, S., Choudhary, A. (2006). Herpes simplex keratitis. *Prog. Retin. Eye Res.* **25**, 355-380.
40. Fatahzadeh, M., Schwartz, R. A. (2007). Human herpes simplex virus infections: Epidemiology, pathogenesis, symptomatology, diagnosis, and management. *J. Am. Acad. Dermatol.* **57**, 737-763.
41. Rouse, B. T., Kaistha, A. (2006). A tale of two  $\alpha$ -herpesviruses: lessons for vaccinologists. *Clin. Infect. Dis.* **42**, 810-817.

42. Rudnick, C., Hoekzema, G. (2002). Neonatal herpes simplex virus infections. *Am. Fam. Physician.* **65**, 1138-1142.
43. Whitley, R. J. (1997). Herpes simplex virus. In: Scheld, W. M., Whitley, R. J., Durack, D. T. (Eds.), "*Infections of the central nervous system*", 2<sup>nd</sup> ed., pp. 73-89. Lippincott-Raven, Philadelphia.
44. Gupta, R., Warren, T., Wald, A. (2007). Genital herpes. *Lancet* **370**, 2127-2137.
45. Lafferty, W. E. (2002). The changing epidemiology of HSV-1 and HSV-2 and implications for serological testing. *Herpes* **9**, 51-55.
46. Holdeman, N. R. (2005). Herpes simplex virus: ocular manifestations. In: Onofrey, B. E., Skorin, L., Holdeman, N. R. (Eds.), "*Ocular Therapeutics Handbook: A Clinical Manual*". 2<sup>nd</sup> ed., pp. 208-210. Lippincott Williams & Wilkins, Philadelphia.
47. Kaye, S. B., Baker, K., Bonshek, R., Maseruka, H., Grinfeld, E., Tullo, A., Easty, D. L., Hart, C. A. (2000). Human herpesviruses in the cornea. *Br. J. Ophthalmol.* **84**, 563-571.
48. Keadle, T. L., Morris, J. L., Pepose, J. S., Stuart, P. M. (2002). CD4+ and CD8+ cells are key participants in the development of recurrent herpetic stromal keratitis in mice. *Microb. Pathogen.* **32**, 255-262.
49. Jirmo, A. C., Nagel, C. H., Bohnen, C., Sodeik, B., Behrens, G. M. (2009). Contribution of direct and cross-presentation to CTL immunity against herpes simplex virus 1. *J. Immunol.* **182**, 283-292.
50. Sarangi, P. P., Sehrawat, S., Suvas, S., Rouse, B. T. (2008). IL-10 and natural regulatory T cells: two independent anti-inflammatory mechanisms in herpes simplex virus-induced ocular immunopathology. *J. Immunol.* **180**, 6297-6306.
51. Stumpf, T. H., Shimeld, C., Easty, D. L., Hill, T. J. (2001). Cytokine production in a murine model of recurrent herpetic stromal keratitis. *Invest. Ophthalmol. Vis. Sci.* **42**, 372-378.
52. Rose, J. K., Whitt, M. A. (2001). Rhabdoviridae: the viruses and their replication. In: Fields, B. N., Knipe, D. M., Howley, P. M., Chanock, R. M., Melnick, J. L., Monath, T. P., Roizman, B., Straus S. E. (Eds.), "*Fields Virology*", 4<sup>th</sup> ed., pp. 1221-1242 Philadelphia: Lippincott Williams & Wilkins; 1221-1242. Lippincott Williams & Wilkins, Philadelphia.
53. Kelley, J. R., Emerson, S. U., Wagner, R. R. (1972). The glycoprotein of vesicular stomatitis virus is the antigen that gives rise to and reacts with neutralizing antibody. *J. Virol.* **10**, 1231-1235.

54. Lefrancois, L., Lyles, D. S. (1983). Antigenic determinants of vesicular stomatitis virus: analysis with antigenic variants. *J. Immunol.* **130**, 394–398.
55. Vandepol, S. B., Lefrancois, L., Holland, J. J. (1986). Sequences of the major antibody binding epitopes of the Indiana serotype of vesicular stomatitis virus. *Virology* **148**, 312–325.
56. Luo, L. H., Li, Y., Snyder, R. M., Wagner, R. R. (1988). Point mutations in glycoprotein gene of vesicular stomatitis virus (New Jersey serotype) selected by resistance to neutralization by epitope-specific monoclonal antibodies. *Virology* **163**, 341–348.
57. Roche S, Albertini AA, Lepault J, Bressanelli S, Gaudin Y. (2008). Structures of vesicular stomatitis virus glycoprotein: membrane fusion revisited. *Cell. Mol. Life Sci.* **65**, 1716-28.
58. Kopecky, S. A., Willingham, M. C., Lyles, D. S. (2001). Matrix protein and another viral component contribute to induction of apoptosis in cells infected with vesicular stomatitis virus. *J. Virol.* **75**, 12169-12181.
59. Gaddy, D. F., Lyles, D. S. (2005). Vesicular stomatitis viruses expressing wild-type or mutant M proteins activate apoptosis through distinct pathways. *J. Virol.* **79**, 4170-4179.
60. Gadaleta, P., Perfetti, X., Mersich, S., Coulombié, F. (2005). Early activation of the mitochondrial apoptotic pathway in vesicular stomatitis virus-infected cells. *Virus Res.* **109**, 65-69.
61. Kopecky, S. A., Lyles, S. D. (2003). Contrasting effects of matrix protein on apoptosis in HeLa and BHK cells infected with vesicular stomatitis virus are due to inhibition of host gene expression. *J. Virol.* **77**, 4658-4669.
62. Faria, P. A., Chakraborty, P., Levay, A., Barber, G. N., Ezelle, H. J., Enninga, J., Arana, C., van Deursen, J., Fontoura, B. M. (2005). VSV disrupts the Rae1/mrnp41 mRNA nuclear export pathway. *Mol. Cell* **17**, 93–102.
63. Schlegel, R., Tralka, T. S., Willingham, M. C., Pastan, I. (1983). Inhibition of VSV binding and infectivity by phosphatidylserine: is phosphatidylserine a VSV-binding site? *Cell* **32**, 639–646.
64. Coil, D. A., Miller, A. D. (2004). Phosphatidylserine is not the cell surface receptor for vesicular stomatitis virus. *J. Virol.* **78**, 10920–10926.
65. Carneiro, F. A., Bianconi, M. L., Weissmüller, G., Stauffer, F., Da Poian, A. T. (2002). Membrane recognition by vesicular stomatitis virus involves enthalpy-driven protein-lipid interactions. *J. Virol.* **76**, 3756–3764.

66. Barber, G. N. (2004). Vesicular stomatitis virus as an oncolytic vector. *Viral Immunol.* **17**, 516-527.
67. Rodríguez, L. L. (2002). Emergence and re-emergence of vesicular stomatitis in the United States. *Virus Res.* **85**, 211-219.
68. Lichty, B. D., Power, A. T., Stojdl, D. F., Bell, J. C. (2004). Vesicular stomatitis virus: re-inventing the bullet. *Trends Mol. Med.* **10**, 210-216.
69. Lichty, B. D., Stojdl, D. F., Taylor, R. A., Miller, L., Frenkel, I., Atkins, H., Bell, J. C. (2004). Vesicular stomatitis virus: a potential therapeutic virus for the treatment of hematologic malignancy. *Hum. Gene Ther.* **15**, 821-831.
70. Balachandran, S., Barber, G. N. (2000). Vesicular stomatitis virus (VSV) therapy of tumors. *IUBMB Life* **50**, 135-138.
71. Balachandran, S., Barber, G. N. (2004). Defective translational control facilitates vesicular stomatitis virus oncolysis. *Cancer Cell* **5**, 51-65.
72. Stojdl, D. F., Lichty, B., Knowles, S., Marius, R., Atkins, H., Sonenberg, N., Bell, J. C. (2000). Exploiting tumor-specific defects in the interferon pathway with a previously unknown oncolytic virus. *Nat. Med.* **6**, 821-825.
73. Masters, P. S., Samuel, C. E. (1983). Mechanism of interferon action: Inhibition of vesicular stomatitis virus replication in human amnion U cells by cloned human leukocyte interferon. II. Effect on viral macromolecular synthesis. *J. Biol. Chem.* **258**, 12026-12033.
74. Barber, G. N. (2005). VSV-tumor selective replication and protein translation. *Oncogene* **24**, 7710-7719.
75. Brady, C. S., Bartholomew, J. S., Burt, D. J., Duggan-Keen, M. F., Glenville, S., Telford, N., Little, A. M., Davidson, J. A., Jimenez, P., Ruiz-Cabello, F., Garrido, F., Stern, P. L. (2000). Multiple mechanisms underlie HLA dysregulation in cervical cancer. *Tissue Antigens* **55**, 401-411.
76. Brender, C., Nielsen, M., Kaltoft, K., Mikkelsen, G., Zhang, Q., Wasik, M., Billestrup, N., Odum, N. (2001). STAT3-mediated constitutive expression of SOCS-3 in cutaneous T-cell lymphoma. *Blood* **97**, 1056-1062.
77. Lensch, M. W., Rathbun, R. K., Olson, S. B., Jones, G. R., Bagby, G. C. Jr. (1999). Selective pressure as an essential force in molecular evolution of myeloid leukemic clones: a view from the window of Fanconi anemia. *Leukemia* **13**, 1784-1789.
78. Moriyama, Y., Nishiguchi, S., Tamori, A., Koh, N., Yano, Y., Kubo, S., Hirohashi, K., Otani, S. (2001). Tumor-suppressor effect of interferon regulatory factor-1 in human hepatocellular carcinoma. *Clin. Cancer Res.* **7**, 1293-1298.

79. Xi, H., Blanck, G. (2000). Interferon regulatory factor-2 point mutations in human pancreatic tumors. *Int. J. Cancer* **87**, 803-808.
80. Balachandran, S., Roberts, P. C., Brown, L. E., Truong, H., Pattnaik, A. K., Archer, D. R., Barber, G. N. (2000). Essential role for the dsRNA-dependent protein kinase PKR in innate immunity to viral infection. *Immunity* **13**, 129-141.
81. Meurs, E., Chong, K., Galabru, J., Thomas, N. S., Kerr, I. M., Williams, B. R., Hovanessian, A. G. (1990). Molecular cloning and characterization of the human double-stranded RNA-activated protein kinase induced by interferon. *Cell* **62**, 379-390.
82. Balachandran, S., Roberts, P. C., Kipperman, T., Bhalla, K. N., Compans, R. W., Archer, D. R., Barber, G. N. (2000). Alpha/beta interferons potentiate virus-induced apoptosis through activation of the FADD/Caspase-8 death signaling pathway. *J. Virol.* **74**, 1513–1523.
83. Abraham, N., Stojdl, D. F., Duncan, P. I., Méthot, N., Ishii, T., Dubé, M., Vanderhyden, B. C., Atkins, H. L., Gray, D. A., McBurney, M. W., Koromilas, A. E., Brown, E. G., Sonenberg, N., Bell J. C. (1999). Characterization of transgenic mice with targeted disruption of 523 the catalytic domain of the double-stranded RNA-dependent protein kinase, PKR. *J. Biol. Chem.* **274**, 5953–5962.
84. Stojdl, D. F., Lichty, B. D., tenOever, B. R., Paterson, J. M., Power, A. T., Knowles, S., Marius, R., Reynard, J., Poliquin, L., Atkins, H., Brown, E. G., Durbin, R. K., Durbin, J. E., Hiscott, J., Bell, J. C. (2003). VSV strains with defects in their ability to shutdown innate immunity are potent systemic anticancer agents. *Cancer Cell* **4**, 263-275.
85. Obuchi, M., Fernandez, M., Barber, G. N. (2003). Development of recombinant vesicular stomatitis viruses that exploit defects in host defense to augment specific oncolytic activity. *J. Virol.* **77**, 8843-8856.
86. Wollmann, G., Rogulin, V., Simon, I., Rose, J. K., van den Pol, A. N. (2010). Some attenuated variants of vesicular stomatitis virus show enhanced oncolytic activity against human glioblastoma cells relative to normal brain cells. *J. Virol.* **84**, 1563-1573.
87. Stojdl, D. F., Abraham, N., Knowles, S., Marius, R., Brasey, A., Lichty, B. D., Brown, E. G., Sonenberg, N., Bell, J. C. (2000). The murine double-stranded RNA-dependent protein kinase PKR is required for resistance to vesicular stomatitis virus. *J. Virol.* **74**, 9580-9585.



88. Hobbs, J. A., Hommel-Berrey, G., Brahmi, Z. (2003). Requirement of caspase-3 for efficient apoptosis induction and caspase-7 activation but not viral replication or cell rounding in cells infected with vesicular stomatitis virus. *Hum. Immunol.* **64**, 82-92.
89. Gallyas, É., Seprényi, G., Sonkoly, E., Mándi, Y., Kemény, L., Megyeri, K. (2006). Vesicular stomatitis virus induces apoptosis in the Wong-Kilbourne derivative of the Chang conjunctival cell line. *Graefe's Arch. Clin. Exp. Ophthalmol.* **244**, 717-724.
90. Kopecky, S. A., Lyles, D. S. (2003). The cell-rounding activity of the vesicular stomatitis virus matrix protein is due to the induction of cell death. *J. Virol.* **77**, 5524-5528.
91. Barbieri, C. E., Pietenpol, J. A. (2006). p63 and epithelial biology. *Exp. Cell Res.* **312**, 695-706.
92. Yang, A., Kaghad, M., Wang, Y., Gillet, E., Fleming, M., Dotsch, V., Andrews, N., Caput, D., McKeon, F. (1998). p63, a p53 homolog at 3q27-29, encodes multiple products with transactivating death-inducing, and dominant-negative activities. *Mol. Cell* **2**, 305-316.
93. Candi, E., Cipollone, R., Rivetti di Val Cervo, P., Gonfloni, S., Melino, G., Knight, R. (2008). p63 in epithelial development. *Cell. Mol. Life Sci.* **65**, 3126-3133.
94. Koster, M. I., Roop, D. R. (2004). The role of p63 in development and differentiation of the epidermis. *J. Dermatol. Sci.* **34**, 3-9.
95. Mills, A. A., Zheng, B., Wang X. J., Vogel, H., Roop, D. R., Bradley A. (1999). p63 is a p53 homologue required for limb and epidermal morphogenesis. *Nature* **398**, 708-713.
96. Yang, A., Schweitzer, R., Sun, D., Kaghad, M., Walker, N., Bronson, R. T., Tabin, C., Sharpe, A., Caput, D., Crum, C., McKeon, F. (1999). p63 is essential for regenerative proliferation in limb, craniofacial and epithelial development. *Nature* **398**, 714-718.
97. Moll, U. M., Slade, N. (2004). p63 and p73: Roles in development and tumor formation. *Mol. Cancer Res.* **2**, 371-386.
98. Strano, S., Rossi, M., Fontemaggi, G., Munarriz, E., Soddu, S., Sacchi, A., Blandino, G. (2001). From p63 to p53 across p73. *FEBS Lett.* **490**, 163-170.
99. Candi, E., Dinsdale, D., Rufini, A., Salomoni, P., Knight, R. A., Mueller, M., Krammer, P. H., Melino, G. (2007). TAp63 and  $\Delta Np63$  in cancer and epidermal development. *Cell Cycle* **6**, 274-285.
100. Trink, B., Osada, M., Ratovitski, E., Sidransky, D. (2007). p63 transcriptional regulation of epithelial integrity and cancer. *Cell Cycle* **6**, 240-245.

101. Tomkova, V., Tomka, M., Zajac, V. (2008). Contribution of p53, p63 and p73 to the developmental diseases and cancer. *Neoplasma* **55**, 177-181.
102. Bénard, J., Douc-Rasy, S., Ahomadegbe, J-C. (2003). TP53 family members and human cancers. *Hum. Mutat.* **21**, 182-191.
103. Flores, E. R. (2007). The roles of p63 in cancer. *Cell Cycle* **6**, 300-304.
104. Levrero, M., De Laurenzi, V., Costanzo, A., Sabatini, S., Gong, J., Wang, J. Y. J. (2000). The p53/p63/p73 family of transcription factors: overlapping and distinct functions. *J. Cell Sci.* **113**, 1661-1670.
105. Gressner, O., Schilling, T., Lorenz, K., Schleithoff, E. S., Koch, A., Schulze-Bergkamen, H., Lena, A. M., Candi, E., Terrinoni, A., Catani, M. V., Oren, M., Melino, G., Krammer, P. H., Stremmel, W., Müller, M. (2005). TAp63 $\alpha$  induces apoptosis by activating signaling via death receptors and mitochondria. *EMBO J* **24**, 2458-2471.
106. Müller, M., Schleithoff, E. S., Stremmel, W., Melino, G., Krammer, P. H., Schilling, T. (2007). One, two, three – p53, p63, p73 and chemosensitivity. *Drug Resist. Update.* **9**, 288-306.
107. Finlan, L. E., Hupp, T. R. (2007). p63: the phantom of the tumor suppressor. *Cell Cycle* **6**, 1062-1071.
108. Dohn, M., Zhang, S., Chen, X. (2001). p63 $\alpha$  and  $\Delta$ Np63 $\alpha$  can induce cell cycle arrest and apoptosis and differentially regulate p53 target genes. *Oncogene* **20**, 3193–3205.
109. Sasaki, Y., Morimoto, I., Ishida, S., Yamashita, T., Imai, K., Tokino, T. (2001). Adenovirus-mediated transfer of the p53 family genes, p73 and p51/p63 induces cell cycle arrest and apoptosis in colorectal cancer cell lines: potential application to gene therapy of colorectal cancer. *Gene Ther.* **8**, 1401-1408.
110. Buzás, K., Miczák, A., Degré, M., Megyeri, K. (2004). Rubella virus infection dysregulates the pattern of p63 expression. *APMIS* **112**, 656-662.
111. Dietrich, J. B. (1997). Apoptosis and anti-apoptosis genes in the Bcl-2 family. *Arch. Physiol. Biochem.* **105**, 125-135.
112. Katoh, I., Aisaki, K-I., Kurata, S-I., Ikawa, S., Ikawa, Y. (2000). p51A (TAp63 $\gamma$ ), a p53 homolog, accumulates in response to DNA damage for cell regulation. *Oncogene* **19**, 3126-3130.
113. Rinne, T., Brunner, H. G., van Bokhoven H. (2007). p63-associated disorders. *Cell Cycle* **6**, 262-268.
114. Irwin, M. S., Kaelin, W. G. (2001). p53 family update: p73 and p63 develop their own identities. *Cell Growth Differ.* **12**, 337-349.

115. Kawasaki, S., Tanioka, H., Yamasaki, K., Connon, C. J., Kinoshita, S. (2006). Expression and tissue distribution of p63 isoforms in human ocular surface epithelia. *Exp. Eye Res.* **82**, 293-299.
116. Arpitha, P., Prajna, N. V., Srinivasan, M., Muthukkaruppan, V. (2008). A subset of human limbal epithelial cells with greater nucleus-to-cytoplasm ratio expressing high levels of p63 possesses slow-cycling property. *Cornea* **27**, 1164-1170.
117. Arpitha, P., Prajna, N. V., Srinivasan, M., Muthukkaruppan, V. (2005). High expression of p63 combined with a large N/C ratio defines a subset of human limbal epithelial cells: implications on epithelial stem cells. *Invest. Ophthalmol. Vis. Sci.* **46**, 3631-3636.
118. Epstein, S. P., Wolosin, J. M., Asbell, P. A. (2005). p63 expression levels in side population and low light scattering ocular surface epithelial cells. *Trans. Am. Ophthalmol. Soc.* **103**, 187-199.
119. Wang, D. Y., Cheng, C. C., Kao, M. H., Hsueh, Y. J., Ma, D. H., Chen, J. K. (2005). Regulation of limbal keratinocyte proliferation and differentiation by TAp63 and  $\Delta$ Np63 transcription factors. *Invest. Ophthalmol. Vis. Sci.* **46**, 3102-3108.
120. Di Iorio, E., Barbaro, V., Ruzza, A., Ponzin, D., Pellegrini, G., De Luca, M. (2005). Isoforms of  $\Delta$ Np63 and the migration of ocular limbal cells in human corneal regeneration. *P. Natl. Acad. Sci. USA* **102**, 9523-9528.
121. Vaux, D. L., Cory, S., Adams, J. M. (1988). Bcl-2 gene promotes haemopoietic cell survival and cooperates with c-myc to immortalize pre-B cells. *Nature* **335**, 440-442.
122. Chao, D. T., Korsmeyer, S. J. (1998). BCL-2 family: regulators of cell death. *Annu. Rev. Immunol.* **16**, 395-419.
123. Borner, C. (2003). The Bcl-2 protein family: sensors and checkpoints for life-or-death decisions. *Mol. Immunol.* **39**, 615-647.
124. Oltvai, Z. N., Milliman, C. L., Korsmeyer, S. J. (1993). Bcl-2 heterodimerizes in vivo with a conserved homolog, Bax, that accelerates programmed cell death. *Cell* **74**, 609-619.
125. Zhou, M., Demo, S. D., McClure, T. N., Crea, R., Bitler, C. M. (1998). A novel splice variant of the cell death-promoting protein BAX. *J. Biol. Chem.* **273**, 1193-11936.
126. Fu, N. Y., Sukumaran, S. K., Kerk, S. Y., Yu, V. C. (2009). Bax $\beta$ : A constitutively active human Bax isoform that is under tight regulatory control by the proteosomal degradation mechanism. *Mol. Cell* **33**, 15-29.

127. Bargou, R. C. (1996). Overexpression of the death-promoting gene Bax-alpha which is downregulated in breast cancer restores sensitivity to different apoptotic stimuli and reduces tumor growth in SCID mice. *J. Clin. Invest.* **97**, 2651-2659.
128. Youle, R. J., Strasser, A. (2008). The BCL-2 protein family: opposing activities that mediate cell death. *Nat. Rev. Mol. Cell Biol.* **9**, 47-59.
129. Kim, H., Hsieh, J. J., Cheng, E. H. (2009). Deadly splicing: Bax becomes Almighty. *Mol. Cell* **33**, 145-146.
130. Cartron, P. F., Oliver, L., Juin, P., Meflah, K., Vallette, F. M. (2004). The p18 truncated form of Bax behaves like a Bcl-2 homology domain 3-only protein. *J. Biol. Chem.* **279**, 11503-11512.
131. Cao, X., Deng, X., May, W. S. (2003). Cleavage of Bax to p18 Bax accelerates stress-induced apoptosis, and a cathepsin-like protease may rapidly degrade p18 Bax. *Blood* **102**, 2605-2614.
132. Boukamp, P., Petrussevska, R. T., Breitkreutz, D., Hornung, J., Markham, A., Fusenig, N. E. (1988). Normal keratinization in a spontaneously immortalized aneuploid human keratinocyte cell line. *J. Cell Biol.* **106**: 761-771.
133. van Bokhoven, H., Brunner, H. G. (2002). Splitting p63. *Am. J. Hum. Genet.* **71**, 1-13.
134. Urist, M. J., Di Como, C. J., Lu, M. L., Charytonowicz, E., Verbel, D., Crum, C. P., Ince, T. A., McKeon, F. D., Cordon-Cardo, C. (2002). Loss of p63 expression is associated with tumor progression in bladder cancer. *Am. J. Pathol.* **161**, 1199-1206.
135. Westfall, M. D., Mays, D. J., Sniezek, J. C., Pietenpol JA. (2003). The  $\Delta$ Np63 $\alpha$  phosphoprotein binds the p21 and 14-3-3 $\sigma$  promoters in vivo and has transcriptional repressor activity that is reduced by Hay-Wells syndrome-derived mutations. *Mol. Cell. Biol.* **23**, 2264-2276.
136. Taddeo, B., Zhang, W., Roizman, B. (2006). The U<sub>L</sub>41 protein of herpes simplex virus 1 degrades RNA by endonucleolytic cleavage in absence of other cellular or viral proteins. *P. Natl. Acad. Sci. USA* **103**, 2827-2832.
137. Matis, J., Kúdelová, M. (2001). Early shutoff of host protein synthesis in cells infected with Herpes simplex viruses. *Acta Virol.* **45**, 269-277.
138. Wysocka, J., Herr, W. (2003). The herpes simplex virus VP16-induced complex: the makings of a regulatory switch. *Trends Biochem. Sci.* **28**, 294-304.
139. Nogueira, M. L., Wang, V. E. H., Tantin, D., Sharp, P. A., Kristie, T. M. (2004). Herpes simplex virus infections are arrested in Oct-1-deficient cells. *P. Natl. Acad. Sci. USA* **101**, 1473-1478.

140. Narayanan, A., Nogueira, M. L., Ruyechan, W. T., Kristie, T. M. (2005). Combinatorial transcription of herpes simplex and varicella zoster virus immediate early genes is strictly determined by the cellular coactivator HCF-1. *J. Biol. Chem.* **280**, 1369-1375.
141. Everett, R. D. (2000). ICP0, a regulator of Herpes simplex virus during lytic and late infection. *BioEssays* **22**, 761-770.
142. Boutell, C., Sadis, S., Everett, R. D. (2002). Herpes simplex virus type 1 immediate early protein ICP0 and its isolated RING finger domain act as ubiquitin E3 ligases *in vitro*. *J. Virol.* **76**, 841-850.
143. Everett, R. D., Murray, J., Orr, A., Preston, C. M. (2007). Herpes simplex virus type 1 genomes are associated with ND10 nuclear substructures in quiescently infected human fibroblasts. *J. Virol.* **81**, 10991-11004.
144. Wilcock, D., Lane, D. P. (1991). Localization of p53, retinoblastoma and host replication proteins at sites of viral replication in herpes-infected cells. *Nature* **349**, 429-431.
145. de Bruyn Kops, A., Knipe, D. M. (1988). Formation of DNA replication structures in herpes virus-infected cells requires a viral DNA binding protein. *Cell* **55**, 857-868.
146. Lilley, C. E., Carson, C. T., Muotri, A. R., Gage, F. H., Weitzman, M. D. (2005). DNA repair proteins affect the lifecycle of herpes simplex virus 1. *P. Natl. Acad. Sci. USA* **102**, 5844-5849.
147. Shirata, N., Kudoh, A., Daikoku, T., Tatsumi, Y., Fujita, M., Kiyono, T., Sugaya, Y., Isomura, H., Ishizaki, K., Tsurumi, T. (2005). Activation of ataxia teleangiectasia-mutated DNA damage checkpoint signal transduction elicited by herpes simplex virus infection. *J. Biol. Chem.* **280**, 30336-30341.
148. Boutell, C., Everett, R. D. (2004). Herpes simplex virus type 1 infection induces the stabilization of p53 in a USP7- and ATM-independent manner. *J. Virol.* **78**, 8068-8077.
149. Wilkinson, D. E., Weller, S. K. (2006). Herpes simplex virus type I disrupts the ATR-dependent DNA-damage response during lytic infection. *J. Cell Sci.* **119**, 2695-7203.
150. Roos, W. P., Kaina, B. (2006). DNA damage-induced cell death by apoptosis. *Trends Mol. Med.* **12**, 440-450.
151. Okada, Y., Osada, M., Kurata, S., Sato, S., Aisaki, K., Kageyama, Y., Kihara, K., Ikawa, Y., Katoh, I. (2002). p53 gene family p51(p63)-encoded, secondary transactivator p51B(TAp63alpha) occurs without forming an immunoprecipitable

- complex with MDM2, but responds to genotoxic stress by accumulation. *Exp. Cell Res.* **276**, 194-200.
152. Petitjean, A., Ruptier, C., Tribollet, V., Hautefeuille, A., Chardon, F., Cavard, C., Puisieux, A., Hainaut, P., Caron de Fromentel, C. (2008). Properties of the six isoforms of p63: p53-like regulation in response to genotoxic stress and cross talk with  $\Delta Np73$ . *Carcinogenesis* **29**, 273-281.
153. Murray-Zmijewski, F., Lane, D. P., Bourdon, J-C. (2006). p53/p63/p73 isoforms: an orchestra of isoforms to harmonise cell differentiation and response to stress. *Cell Death Differ.* **13**, 962-972.
154. Schlottmann, K., Schölmerich, J. (2000). BCL-2 family members and mitochondria. In: Schunkert, H., Riegger, G. A. J. (Eds.), "*Apoptosis in cardiac biology*", 1<sup>st</sup> ed., pp. 71-91. Springer, Berlin.
155. Diao, L., Zhang, B., Fan, J., Gao, X., Sun, S., Yang, K., Xin, D., Jin, N., Geng, Y., Wang, C. (2005). Herpes virus proteins ICP0 and BICP0 can activate NF-kappaB by catalyzing I kappa B alpha ubiquitination. *Cell. Signal.* **17**, 217-229.
156. Meulmeester E, Maurice MM, Boutell C. (2005). Loss of HAUSP-mediated deubiquitination contributes to DNA damage-induced destabilization of Hdmx and Hdm2. *Mol. Cell* **18**, 565-576.
157. Yedowitz, J. C., Blaho, J. A. (2005). Herpes simplex virus 2 modulates apoptosis and stimulates NF-kappaB nuclear translocation during infection in human epithelial Hep-2 cells. *Virology* **342**, 297-310.
158. Fusenig, N. E., Boukamp, P. (1998). Multiple stages and genetic alterations in immortalization, malignant transformation, and tumor progression of human skin keratinocytes. *Mol. Carcinog.* **23**, 144-158.
159. Itoh, M., Chiba, H., Noutomi, T., Takada, E., Mizuguchi, J. (2000). Cleavage of Bax-alpha and Bcl-x(L) during carboplatin-mediated apoptosis in squamous cell carcinoma cell line. *Oral Oncol.* **36**, 277-285.
160. Tavolari, S., Bonafè, M., Marini, M., Ferreri, C., Bartolini, G., Brighenti, E., Manara, S., Tomasi, V., Laufer, S., Guarnieri, T. (2008). Licofelone, a dual COX/5-LOX inhibitor, induces apoptosis in HCA-7 colon cancer cells through the mitochondrial pathway independently from its ability to affect the arachidonic acid cascade. *Carcinogenesis* **29**, 371-380.